Science of the Total Environment 904 (2023) 166746

Contents lists available at ScienceDirect

Science of the Total Environment

journal homepage: www.elsevier.com/locate/scitotenv

A new spatial estimation model and source apportionment of aliphatic hydrocarbons in coastal surface sediments of the Nayband Bay, Persian Gulf

Sadegh Partani [a,*], Ali Danandeh Mehr [b,c], Mohsen Maghrebi [d], Rouzbeh Mokhtari [e], Hans-Peter Nachtnebel [f], Ricardo Hideo Taniwaki [g], Amin Arzhangi [a]

[a] Civil Engineering Department, Faculty of Engineering, University of Bojnord, Bojnord, Iran
[b] Civil Engineering Department, Antalya Bilim University, Antalya 07190, Turkey
[c] MEU Research Unit, Middle East University, Amman 11831, Jordan
[d] School of Environment, College of Engineering, University of Tehran, Tehran, 1417853111, Iran
[e] Kargosha Urban Human Ecology Research Group, Tehran, Iran
[f] Institute of Water Management, Hydrology and Hydraulic Engineering, Department of Water-Atmosphere-Environment, University of BOKU, A-1190 Vienna, Austria
[g] Engineering, Modelling and Applied Social Sciences Center, Federal University of ABC, Av. dos Estados, 5001, Santo Andre, SP, Brazil

HIGHLIGHTS

- The study identifies hydrocarbon pollution sources in Nayband Bay, a marine park with mangroves in the Persian Gulf.
- Three indices are used to identify hydrocarbon origin in the bay's coastal area, and anthropogenic sources are found to be the primary contributor.
- An interpolation method estimates hydrocarbon concentrations in surface sediments, reducing sampling stations and low-frequency monitoring.
- The study uses statistical methods to evaluate proposed methods and suggests combining results from various scenarios for accurate and reliable hydrocarbon measurement.

GRAPHICAL ABSTRACT

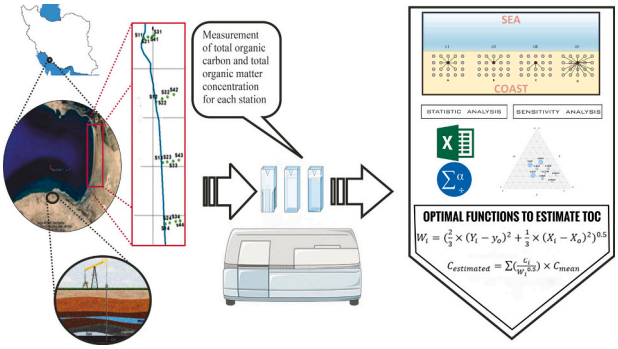

ARTICLE INFO

Editor: Paromita Chakraborty

Keywords:
Hydrocarbons
Coastal sediment
Petrogenic source
Mangrove
Persian Gulf

ABSTRACT

Hydrocarbons, originating from oil and gas industries, are considered a potential risk for Nayband Bay, a natural marine park with extended mangroves, located on the north coastlines of the Persian Gulf, Iran. This paper determines the potential sources and spatial distribution of hydrocarbons, especially aliphatic hydrocarbons (AHCs), in Nayband Bay through the simultaneous application of three indices in the coastline surface sediments. To this end, a field study was conducted in the inter-tidal coastal zones and wetlands. Sediment samples were taken from surface layers along four transects with four sampling points at different distances from the gulf. The hydrocarbon compounds of the samples including AHCs, total petroleum hydrocarbons, and heavy metals (Ni, V as crude oil indicators) were analyzed and classified to discover the pollution indicators. Pearson pairwise correlation and cluster analyses along with pollution indices were employed to describe the spatial distribution pattern of hydrocarbons, identify hot spots, and determine the potential origin of AHCs. Different interpolation

* Corresponding author.
E-mail address: s_partani@ub.ac.ir (S. Partani).

https://doi.org/10.1016/j.scitotenv.2023.166746
Received 16 July 2023; Received in revised form 29 August 2023; Accepted 30 August 2023
Available online 9 September 2023

scenarios based on topographic and oceanic features were proposed to detect the spatial dynamics of AHCs. The results revealed that hydrocarbons mainly originated from anthropogenic sources including oil and gas industries located far from the affected area. It was also concluded that the long-distance pollution transfer was based on oceanic currents and wind direction in the bay. The proposed scenarios showed that the mean concentration values of total organic carbon and total organic material vary in the range 0.19 ppm to 0.4 ppm and 2.88 ppm to 3.20 ppm, respectively.

1. Introduction

Recent studies have shown increasing environmental pollution and distortion in ecosystems mainly due to emanating from human activities (Zhang et al., 2022a, 2022b; Fang et al., 2023). Accordingly, different methods for pollutant monitoring, sampling, and measurement are suggested (e.g., Dai et al., 2022; Lin et al., 2021; Li et al., 2022). For example, increased pollution and environmental degradation of the Caspian Sea was investigated by Modabberi et al. (2020) vial long-term satellite data analysis. Li et al. (2021) monitored and quantified the effects of the canopy and understory global nitrogen addition on the biomass and morphology of fine roots in a temperate deciduous forest in central China through an innovative analysis of soil samples. The study illustrated that fine root morphology was mostly affected during the growing season. Zhang et al. (2023) demonstrated a significant alteration in soil chemical elements owing to the reclamation of coastal wetlands in China. More recently, Yang et al. (2023) investigated the effect of a large-scale vegetation restoration project on the Loess Plateau and concluded that the project has increased the ecosystem carbon stocks. The authors highlighted that carbon stored in roots strongly contributes to soil organic matter formation markedly.

Focusing on marine ecosystems, numerous studies have investigated origins of pollutant, particularly hydrocarbons, and the ways to mitigate hazardous materials from these habitats (Xu et al., 2022a; Kashif et al., 2023; Nie et al., 2023). For example, land-plant debris that is directly washed into the lakes were considered as one of the origins of hydrocarbons (Wei et al., 2020). So, the biogenic sources may appear in lakes with wide spread of marine plants (Pu et al., 2017). Less amount of low molecular weight n-alkenes also have been reported in soil and sediments of Niger Delta, Nigeria (Ekpo et al., 2005) and Lake Erie (Lu and Meyers, 2009). The aliphatic hydrocarbons (AHCs) are usually assigned to the degradation of plant leaves and biological activities (Pu et al., 2017; Brink, 2022). Marine algae, plankton (Duan et al., 2019), cyanobacteria, marine animals and plants were diagnosed as the sources of AHCs in sub-tropical coastal zone of Asaluyeh, Iran (Rostami et al., 2019). In areas close to port entrance, commercial marine transportation has been considered as hydrocarbon pollution factors that increase the concentration of AHCs (Wang et al., 2006).

Tropical and subtropical gulfs, such as Persian Gulf, are among vulnerable marine habitats requiring protection against anthropogenic pollution (Sheppard et al., 2010; Sale et al., 2011). The Persian Gulf ecosystem faces threats from various sources, including the outbreak of wars, the presence of refineries and oil platforms around the Gulf, the discharge of chemicals and oil products, tankers transportation, and dispose of wastes into the gulf (Sheppard et al., 2010). In addition, rising temperature due to climate change has been introduced as another detrimental reason for Gulf's inhabitants (Noori et al., 2017, 2019). Geochemical characteristics of geological formations showed the origins of hydrocarbons which have gotten released into underground water resources probably (Alizadeh et al., 2018). Hydrocarbon source apportionment studies are important where there are multiple sources and it is difficult to diagnose the dominant source (Balgobin and Ramroop Singh, 2019; Commendatore et al., 2012; Xu et al., 2022b).

Several recent studies have investigated the sources of hydrocarbon pollutants over the Persian Gulf (e.g., Tolosa et al., 2005; Mohebbi nozar et al., 2014; Mehdinia et al., 2015; Akhbarizadeh et al., 2016; Keshavarzifard et al., 2017; Rastegari Mehr et al., 2020). For instance, the analysis of the hydrocarbons in surface sediments from the northern parts of the Strait of Hormuz has concluded that the hydrocarbons were originated by both petrogenic and pyrogenic sources (Mohebbi nozar et al., 2014). The sampling process was carried out during the highest and lowest tidal times, in both wet and dry seasons. To determine the probable sources of hydrocarbons, statistical methods, such as principal component analysis (PCA) and multivariable regression were used. The potential sources of hydrocarbons have also been inspected in the coastal water and surface sediments of Kharg Island, a main Iranian oil terminal in the Persian Gulf, using PCA (Rushdi et al., 2017). The findings revealed that the petrogenic sources were the main contributor of hydrocarbons in the island. In the southern coastlines of the gulf, the chemical analysis of surface sediment samples showed that probable sources are both biogenic and petrogenic (Tolosa et al., 2005). Rostami et al. (2019) investigated the source of hydrocarbons in the surface sediments of the Pars Special Economy Energy Zone (PSEEZ), located in the north coastlines of the Persian Gulf, through analysing 15 sampling points. The authors reported that the hydrocarbons are mainly originated by gas and oil industries in the PSEEZ. The PCA was also used by Soliman et al. (2019) to determine the probable sources of hydrocarbons in the central parts of the Persian Gulf, close to Qatar. Different sediment samples were collected at different seasons at several stations. Like the earlier studies, the findings indicated that both petrogenic and pyrogenic sources were the main contributors of hydrocarbons while the pyrogenic was slightly dominant. More recently, Samsami et al. (2022) collected samples from four sites exposed to the human activities such as oil and gas production and showed that the organic matters are mainly originated by petrogenic sources.

Our review showed that hydrocarbon pollutants in the Persian Gulf not only originates from petrogenic sources but also come from biogenic organic compounds. Moreover, petrogenic contamination based on oil and gas projects and petrochemical industries were considered as toxic components and polycyclic aromatic hydrocarbons (PAHs) in coastal sediments (Rostami et al., 2019). Therefore, petrogenic hydrocarbons usually mix with the biogenic organic compounds in the coastal areas. This may result in misleading to detect of anthropogenic sources of hydrocarbons, mainly oil and gas activities, in the gulf. In this regards, simultaneous application of three or more indices may be considered to properly clarify such arguments (Mahmoodi et al., 2012; Resmi et al., 2016).

The Nayband Bay, located in the northern coastal zone of the Persian Gulf, has a unique semi-tropical ecosystem, including a valuable mangrove community, but now it is increasingly facing threats from different pollution sources. In this study, we aimed to discover the extent and sources of hydrocarbon pollution in the sediment of the coastline along the Nayband Bay. Differing from the earlier studies, we introduce a novel geospatial approach to estimate hydrocarbon concentrations in small areas suffering from missing data or low-frequency monitoring stations. The proposed method is based on the distance between the available stations and the direction of wave movement. By combining this estimation method with hydraulic characteristics and pollution indices, this study effectively identifies the origin of hydrocarbons in ecotones and coastal areas. Therefore, the attained insights are expected not only contribute to the protection and conservation of this specific bay but may provide broader understanding of pollution dynamics in similar coastal environments around the world.

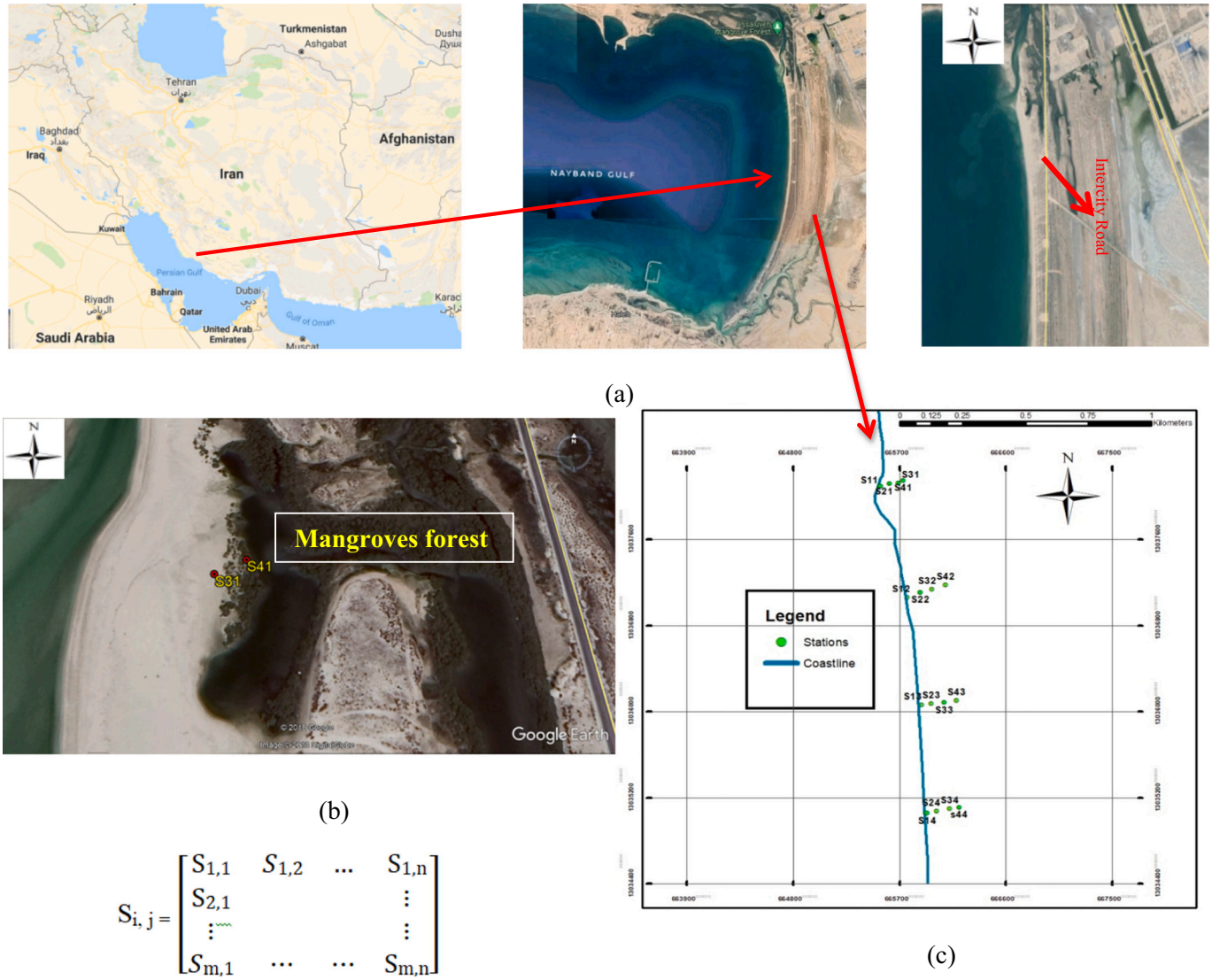

Fig. 1. Location of Nayband Bay and sediments sampling site; a) The plan of study area; b) Sampling stations which are located in salt marsh; c) Sampling stations coordination; d) matrix of sampling points based on map.

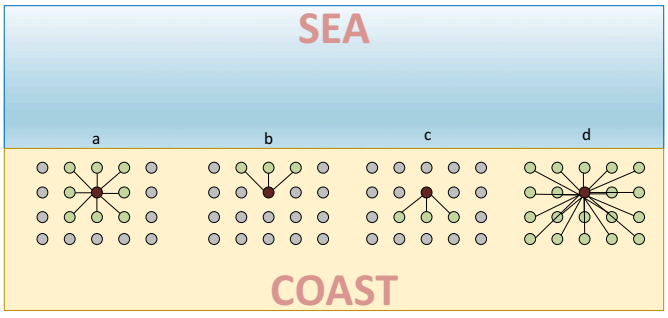

Fig. 2. Calculation pattern for mean concentration scenarios: a) Neighborhoods (C_I), b) Sea to Coast (C_{II}), c) Coast to Sea (C_{III}), and d) Total (C_{IV}).

2. Material and methods

2.1. Study area

Nayband Bay (Fig. 1) with an area of 19,500 ha and a mean depth of 6 m is located on the north coast of the Persian Gulf. The bay is home to a variety of aquatic species, marine mammals, endangered reptiles such as the green and eagle tip turtles, and a number of aquatic birds (Owfi, 2018). It includes a coastal wetland that is famous for its rich ecosystem with an area of about 27,000 ha. It was assigned as a natural protected zone by the World Commission of Protected Areas, which is a branch of the International Union of Conservation of Nature in 2004. Coastal environments in the bay constitute a territory with dense mangrove that includes several species (Davari et al., 2010). The salt marshes are hosting some endangered species of mangroves including Avecennia

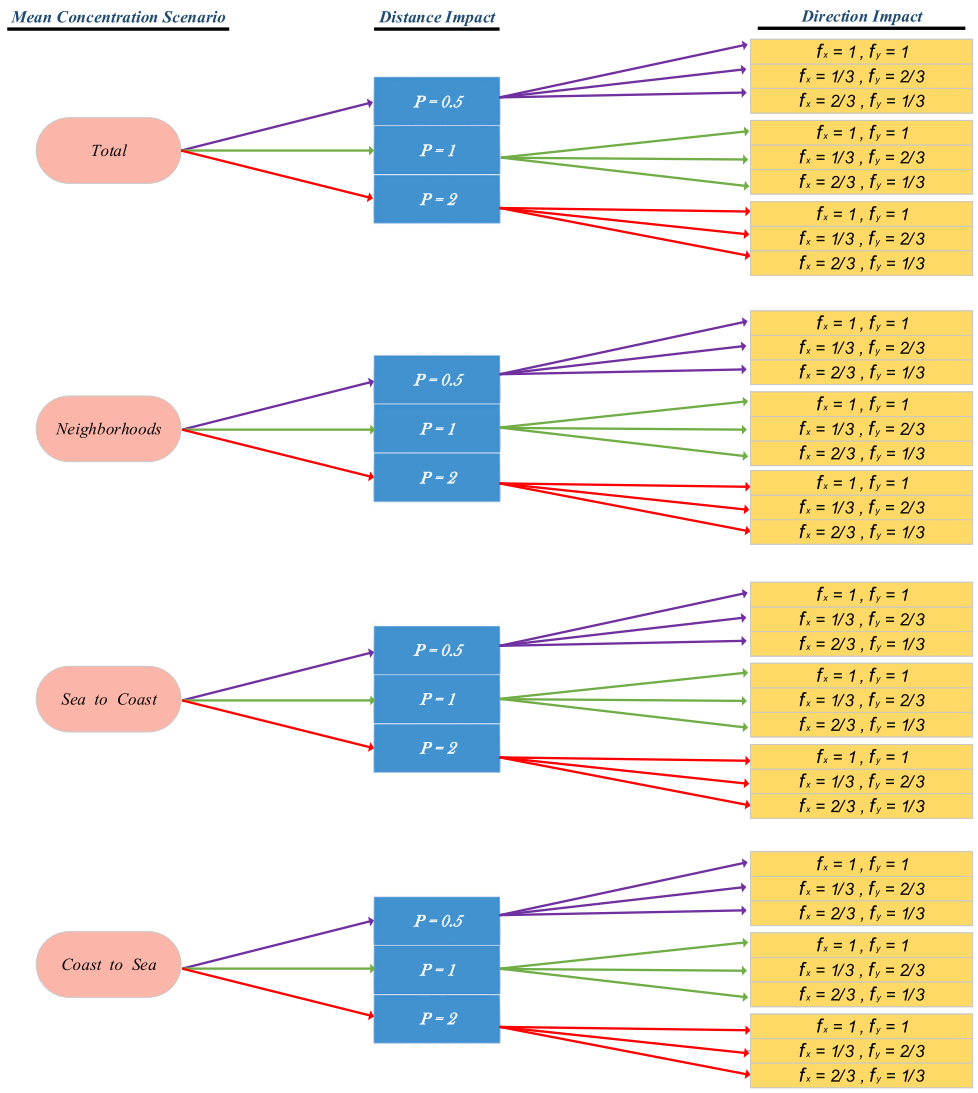

Fig. 3. Flow diagram of the estimation scenarios.

Table 1
C_{mean} values (ppm) attained for TOC at different scenarios.

Station	Neighborhoods	Sea to Coast	Coast to Sea	Total
s11	0.25	–	0.24	0.33
s12	0.29	–	0.30	0.32
s13	0.32	–	0.34	0.31
s14	0.39	–	0.37	0.32
s21	0.25	0.19	0.29	0.32
s22	0.31	0.27	0.34	0.32
s23	0.33	0.33	0.35	0.31
s24	0.38	0.36	0.39	0.32
s31	0.27	0.24	0.30	0.32
s32	0.34	0.30	0.34	0.32
s33	0.33	0.34	0.35	0.31
s34	0.39	0.37	0.39	0.31
s41	0.28	0.29	–	0.31
s42	0.36	0.34	–	0.32
s43	0.33	0.35	–	0.31
s44	0.40	0.39	–	0.31

Table 2
Same as Table 1 but for TOM.

Station	Neighborhoods	Sea to Coast	Coast to Sea	Total
s11	3.05	–	3.01	3.07
s12	3.09	–	2.99	3.09
s13	3.17	–	3.12	3.10
s14	3.07	–	3.12	3.08
s21	3.20	3.31	3.14	3.08
s22	3.09	3.20	3.08	3.09
s23	3.10	3.15	2.98	3.11
s24	3.02	3.17	2.91	3.08
s31	3.12	3.01	3.24	3.09
s32	3.07	2.99	3.15	3.09
s33	3.03	3.12	2.96	3.11
s34	2.99	3.12	2.88	3.11
s41	3.14	3.14	–	3.08
s42	3.11	3.08	–	3.09
s43	2.97	2.98	–	3.11
s44	2.93	2.91	–	3.12

marina and *Rhizophora mucronata* (Duke et al., 2010; Usman et al., 2013). The high risk of oil pollution in the coastal area of Nayband Bay, as a natural national marine park has led most environmental scientists to study the area providing a scientific basis for preserving nature (Davoodi et al., 2017; Owfi, 2018; Dashtbozorg et al., 2019). The study area is in the vicinity of one of the largest oil and gas industrial zones including the giant on-shore and off-shore complexes of Iranian oil companies, namely Asaluyeh, in the world (Ashournejad et al., 2019). Gas extraction activities and drilling rigs dominantly are laid down offshore and refineries and terminals as well onshore. Prosperity in the

Table 3
The distance dimensionless weight between the stations considering $f_x = 1/3$ and $f_y = 2/3$.

	S_{11}	S_{12}	S_{13}	S_{14}	S_{21}	S_{22}	S_{23}	S_{24}	S_{31}	S_{32}	S_{33}	S_{34}	S_{41}	S_{42}	S_{43}	S_{44}
S_{11}	0.0	397.9	777.2	1162.8	20.8	386.4	782.4	1162.4	56.6	386.3	782.7	1158.3	69.2	383.8	783.6	1156.0
S_{12}		0.0	381.0	767.5	395.4	35.4	384.6	765.7	409.5	64.1	384.9	760.8	417.3	98.9	387.0	758.2
S_{13}			0.0	386.5	775.8	399.4	36.4	385.3	790.5	410.0	64.8	382.1	798.2	429.4	94.7	381.5
S_{14}				0.0	1161.9	785.5	386.8	34.3	1177.0	794.8	394.2	64.7	1184.7	811.8	404.6	86.8
S_{21}					0.0	382.2	780.0	1160.9	37.1	380.5	779.6	1166.0	50.2	376.2	779.7	1153.5
S_{23}						0.0	400.1	782.3	393.4	29.1	398.1	776.2	400.4	63.8	397.6	772.7
S_{23}							0.0	382.3	793.2	408.3	28.7	376.3	800.4	425.0	58.7	373.7
S_{24}								0.0	1175.0	790.4	387.3	30.6	1182.4	806.1	395.3	52.7
S_{31}									0.0	389.1	791.5	1169.5	13.2	381.6	790.3	1166.1
S_{32}										0.0	404.2	783.2	395.2	34.8	401.6	778.9
S_{33}											0.0	379.1	798.3	418.9	30.0	374.8
S_{34}												0.0	1176.6	797.8	384.9	22.1
S_{41}													0.0	386.6	796.7	1173.0
S_{42}														0.0	413.9	792.6
S_{43}															0	378.9
S_{44}																0

Table 4
Same as Table 3 for $f_x = 2/3$ and $f_y = 1/3$.

	S_{11}	S_{12}	S_{13}	S_{14}	S_{21}	S_{22}	S_{23}	S_{24}	S_{31}	S_{32}	S_{33}	S_{34}	S_{41}	S_{42}	S_{43}	S_{44}
S_{11}	0.0	295.4	561.2	832.8	29.4	301.1	575.4	840.2	77.0	316.8	586.2	845.5	92.5	336.4	599.6	850.9
S_{12}		0.0	270.5	544.3	286.9	44.5	280.5	547.9	290.6	84.0	291.1	551.2	295.3	129.4	307.0	555.8
S_{13}			0.0	273.9	555.6	282.7	51.4	279.0	561.1	293.7	91.5	286.8	565.5	315.3	133.3	296.2
S_{14}				0.0	828.5	555.4	274.8	48.3	834.9	562.7	285.3	90.2	839.5	577.9	302.1	120.7
S_{21}					0.0	288.5	567.3	834.2	48.1	301.0	576.2	838.1	63.8	317.5	587.8	842.5
S_{23}						0.0	284.7	555.2	284.8	39.7	289.2	555.2	287.2	85.1	299.2	557.3
S_{23}							0.0	270.8	568.5	288.7	40.2	271.1	571.6	303.2	82.0	275.4
S_{24}								0.0	837.9	559.1	274.6	42.0	841.5	570.6	284.9	72.5
S_{31}									0.0	291.0	574.0	839.4	15.8	300.8	582.2	842.0
S_{32}										0.0	287.7	556.0	291.2	45.4	292.1	556.0
S_{33}											0.0	268.6	576.0	296.3	41.8	268.5
S_{34}												0.0	842.3	564.2	272.8	30.5
S_{41}													0.0	298.6	583.1	844.3
S_{42}														0.0	294.2	561.7
S_{43}															0.0	268.0
S_{44}																0.0

Table 5
Same as Table 3 for $f_x = 1$ and $f_y = 1$.

	S_{11}	S_{12}	S_{13}	S_{14}	S_{21}	S_{22}	S_{23}	S_{24}	S_{31}	S_{32}	S_{33}	S_{34}	S_{41}	S_{42}	S_{43}	S_{44}
S_{11}	0	495.6	958.6	1430.3	36.0	489.9	971.2	1434.3	95.6	499.6	977.9	1434.1	115.5	510.3	986.7	1435.4
S_{12}		0.0	467.2	940.9	488.5	56.9	476.0	941.6	502.2	105.6	482.6	939.5	511.3	162.9	494.0	940.1
S_{13}			0.0	473.7	954.2	489.3	63.0	475.7	969.4	504.3	112.2	477.8	978.3	532.7	163.5	483.0
S_{14}				0.0	1427.0	962.0	474.4	59.2	1443.1	973.8	486.7	111.0	1452.0	996.4	504.9	148.6
S_{21}					0.0	478.9	964.5	1429.5	60.7	485.2	969.4	1428.1	81.2	492.3	976.4	1428.4
S_{23}						0.0	491.1	959.3	485.7	49.2	492.1	954.3	492.7	106.3	497.6	952.7
S_{23}							0.0	468.5	975.8	500.0	49.4	463.8	983.5	522.1	100.8	464.2
S_{24}								0.0	1443.1	968.2	474.8	52.0	1451.3	987.6	487.3	89.6
S_{31}									0.0	485.8	977.7	1439.5	20.6	485.8	981.6	1438.3
S_{32}										0.0	496.1	960.6	490.9	57.2	496.6	957.0
S_{33}											0.0	464.6	984.4	513.1	51.5	461.1
S_{34}												0.0	1447.0	977.1	471.8	37.7
S_{41}													0.0	488.5	987.3	1445.3
S_{42}														0.0	507.8	971.4
S_{43}															0.0	464.1
S_{44}																0.0

Gulf region including Iran and Gulf countries is triggered by oil and gas extraction, sometimes in a competitive manner among riparian states.

2.2. Sampling and measurements

Surface coastal sediment samples were taken from 16 stations with structured designs in two parallel and perpendicular lines (network pattern) on April 10, 2019. According to Fig. 1, there are four transects; each one includes four stations. Total organic matter (TOM), total organic carbon (TOC), and *n*-alkanes were measured in each sample. Each sample was around 500 g, taken from 5.0 to 10.0 cm depth. Samples were stored in cooling boxes at 4 °C to avoid any ongoing chemical processes of organic compounds during transportation (Fisher et al., 2015). To catch an appropriate vision of the spatial distribution of petroleum hydrocarbons, sampling was carried out in two directions, Longitudinal and perpendicular to the coastline as shown in Fig. 1. In-situ measurements were conducted for climatological parameters such as air temperature etc. For gas chromatography and mass spectrometry an Agilent 7890 device was used.

To investigate the general features of hydrocarbons' content and their geographical distribution, a cluster analysis was employed. The indices that were used to describe the hydrocarbons' origin were based

Table 6
GPS locations and indices of n-alkanes in the coastal sediments.

Station	GPS locations	Tn-A (ppm)	LMW/HMW	Pri/Phy	CPI	n-C17/Pri	n-C18/Phy	TOM	TOC
S11	665,482.00 m E 3,037,084.00 m N	7.33	11.95	1.22	1.14	1.58	0.67	3.5	0.11
S12	665,609.00 m E 3,036,605.00 m N	4.41	12.81	1.02	1.29	2.09	1.04	3.12	0.27
S13	665,643.00 m E 3,036,139.00 m N	6.13	11.98	1.28	1.47	1.58	0.87	2.97	0.42
S14	665,669.00 m E 3,035,666.00 m N	5.45	16.93	1.31	0.78	1.43	0.92	3.37	0.3
S21	665,518.00 m E 3,037,085.00 m N	5.08	12.21	0.78	1.25	1.48	0.36	2.9	0.21
S22	665,661.00 m E 3,036,628.00 m N	4.29	12.83	1.03	1.32	1.83	1.11	3.12	0.27
S23	665,706.00 m E 3,036,139.00 m N	6.15	11.86	1.32	1.49	1.53	0.91	2.96	0.43
S24	665,728.00 m E 3,035,671.00 m N	5.88	15.56	1.15	1.01	1.31	0.71	3.27	0.31
S31	665,575.00 m E 3,037,106.00 m N	5.66	10.63	1.24	1.23	1.64	0.89	3.16	0.31
S32	665,709.00 m E 3,036,639.00 m N	4.39	12.81	1.02	1.3	2.06	1.05	3.12	0.27
S33	665,755.00 m E 3,036,145.00 m N	6.16	11.79	1.34	1.5	1.51	0.93	2.95	0.44
S34	665,779.00 m E 3,035,681.00 m N	7.65	12.67	0.92	1.51	1.03	0.39	2.87	0.33
S41	665,593.00 m E 3,037,116.00 m N	5.5	18.56	0.36	0.69	27.78	0.45	3.35	0.33
S42	665,763.00 m E 3,036,658.00 m N	4.64	12.78	0.99	1.26	2.59	0.93	3.13	0.27
S43	665,806.00 m E 3,036,152.00 m N	6.15	11.87	1.32	1.49	1.53	0.9	2.96	0.43
S44	665,816.00 m E 3,035,688.00 m N	8.02	12.32	0.9	1.58	0.99	0.36	2.79	0.34
Max	–	8.02	18.56	1.34	1.58	27.78	1.11	3.5	0.44
Min	–	4.29	10.63	0.36	0.69	0.99	0.36	2.79	0.11
Mean	–	5.81	13.1	1.08	1.27	3.25	0.78	3.1	0.32

Tn-A: Total n-alkanes = sum of n-alkanes within the range of C_9-C_{35}.
LMW/HMW = sum of LMW n-alkanes (C_9-C_{22}) over of HMW n-alkanes (C_{23}-C_{35}) (Vaezzadeh et al., 2015).
Pri/Phy = ratio of pristane over phytane.
CPI $_{long\ chain}$ = ½[(∑odd C_{25} to C_{31}) / (∑odd C_{24} to C_{30}) + (∑odd C_{25} to C_{31}) / (∑odd C_{26} to C_{32})] (Harvey and Taylor, 2017).
n-C_{17}/Pri = ratio of C_{17} n-alkane over pristane.
n-C_{18}/Pri = ratio of C_{18} n-alkane over phytane.
TOM: Total organic matter.
TOC: Total organic carbon.

on LMW/HMW (Madany et al., 1998), Pri/Phy (Steinhauer and Boehm, 1992), CPI (Marzi et al., 1993), n-C17/Pri, and n-C18/Phy (Colombo et al., 1989). Zoning of derived indices was carried out with the ordinary type of Kriging interpolation to illustrate a snapshot of their spatial variation. It helped to describe the behavior of indices and n-alkanes and discuss their geographical sources. In addition, the identification of trends along transects and heterogeneity in data and hot spot detections could be figured out by geospatial multi-variable statistical analysis on measured data and confirmed the effects of some sources.

2.3. Quality control/quality assurance

Quality control was carried out to increase the reliability of the results and reduce the possible errors during field study and analytical procedures. To this end, the reagent-free deionized water as blank samples (Gries, 2007; USEPA, 1995), duplicates/replicates sampling, and analysis of the standard references were used. Duplicate sample analysis was prepared for 15 % (USEPA, 1995) of the total samples which provides a measure of processing and analytical precision.

Field blank samples that were collected during field sampling cruises, were processed in parallel to samples and followed the same analytical scheme. The granular analysis of surface sediment samples through this research showed that the grain size distribution for all stations referred to sandy clay (Flemming, 2000). All samples were classified in sandy fraction dominantly with a low contribution of clay particles.

2.4. Statistical analysis

All the data was analyzed using Pearson pairwise correlation analysis (PPCA). The PPCA between all stations and n-alkanes was conducted to find out the relation and trends in hydrocarbon levels. The Anderson-Darling test (de Arruda-Santos et al., 2018) was applied to evaluate the normal distribution in n-alkanes prior to the multivariable statistical analysis (significance level was considered at p-value ≤ 0.05). Moreover, cluster analysis was applied for stations and AHCs individually to explore if one station or one index could have different variations or not (the variation might be associated with sand and organic matter content).

2.5. The proposed inter-estimation approach to reduce the number of stations

In the germane literature, two interpolation methods, namely certain and geospatial interpolations are used. While the former is a method in which the results are the same or so close to the lab results, in the latter, geo-correlation between the stations is used to estimate the desired parameter in stations. An important point in geospatial methods, such as

Table 8
Calculation of statistical indicators for TOC.

MCS	P	fx	fy	R2	RMSE	RSS	TSS	VAR_U	B1po	B1op	RSR
Coast to Sea	0.50	0.33	0.67	0.857	0.308	1.002	0.058	9E−05	0.137	13.57	0.083
		0.67	0.33	0.833	0.290	1.012	0.098	5E−05	0.074	13.57	0.084
		1.00	1.00	0.846	0.295	1.042	0.098	3E−05	0.063	15.83	0.087
	1.00	0.33	0.67	0.383	0.314	1.186	0.098	2E−06	0.021	47.50	0.099
		0.67	0.33	0.341	0.315	1.193	0.098	2E−06	0.011	95.00	0.099
		1.00	1.00	0.344	0.316	1.200	0.098	9E−07	0.011	95.00	0.100
	2.00	0.33	0.67	0.039	0.319	1.220	0.098	2E−08	–	–	0.102
		0.67	0.33	0.020	1.220	1.220	0.098	9E−09	–	–	0.102
		1.00	1.00	0.025	0.319	1.220	0.098	3E−09	–	–	0.102
Sea to Coast	0.50	0.33	0.67	0.612	0.308	1.140	0.058	9E−05	0.137	7.30	0.095
		0.67	0.33	0.572	0.310	1.150	0.058	7E−05	0.123	8.11	0.096
		1.00	1.00	0.590	0.333	1.179	0.058	1E−06	0.014	73.00	0.111
	1.00	0.33	0.67	0.434	0.331	1.319	0.058	3E−06	0.027	36.50	0.110
		0.67	0.33	0.368	0.332	1.325	0.058	2E−06	0.014	73.00	0.110
		1.00	1.00	0.388	0.333	1.331	0.058	1E−06	0.014	73.00	0.111
	2.00	0.33	0.67	0.082	0.335	1.351	0.058	2E−08	–	–	0.113
		0.67	0.33	0.041	0.336	1.351	0.058	8E−09	–	–	0.113
		1.00	1.00	0.053	0.336	1.351	0.058	3E−09	–	–	0.113
Neighborhoods	0.50	0.33	0.67	0.343	0.276	1.215	0.116	4E−04	0.216	4.63	0.076
		0.67	0.33	0.323	0.276	1.221	0.116	4E−04	0.216	4.63	0.076
		1.00	1.00	0.274	0.285	1.295	0.116	2E−04	0.182	5.50	0.081
	1.00	0.33	0.67	0.337	0.320	1.632	0.116	7E−06	0.034	29.33	0.102
		0.67	0.33	0.325	0.321	1.643	0.116	4E−06	0.023	44.00	0.103
		1.00	1.00	0.325	0.322	1.659	0.116	3E−06	0.023	44.00	0.104
	2.00	0.33	0.67	0.088	0.326	1.701	0.116	2E−08	–	–	0.106
		0.67	0.33	0.050	0.326	1.702	0.116	1E−08	–	–	0.106
		1.00	1.00	0.061	0.326	1.702	0.116	4E−09	–	–	0.106
Total	0.50	0.33	0.67	0.438	0.233	0.865	0.116	7E−05	0.097	10.35	0.054
		0.67	0.33	0.350	0.231	0.854	0.116	5E−05	0.083	12.05	0.053
		1.00	1.00	0.397	0.248	0.983	0.116	4E−05	0.073	13.75	0.120
	1.00	0.33	0.67	0.398	0.316	1.602	0.116	3E−06	0.022	46.32	0.176
		0.67	0.33	0.339	0.318	1.614	0.116	2E−06	0.016	62.86	0.101
		1.00	1.00	0.354	0.320	1.638	0.116	1E−06	0.011	88.00	0.102
	2.00	0.33	0.67	0.038	0.316	1.700	0.116	3E−06	0.022	46.32	0.100
		0.67	0.33	0.018	0.326	1.702	0.116	1E−08	–	–	0.106
		1.00	1.00	0.023	0.326	1.702	0.116	4E−09	–	–	0.106

MCS = Mean Concentration Scenario; RSME = Root Mean Squared Error; RSS = Residual sum of squares.
TSS = Total sum of squares; VAR_U = Sample variance, uncorrected; β1 = Slope of SMA regression.
RSR = Root Mean Standard Deviation Ratio.

geo-Kriging method (Rossi et al., 1994), is the marked difference between the estimated and real measured amounts (Abbasnejadfard et al., 2021). Based on horizontal and vertical distance between the stations, a new geospatial interpolation method to estimate TOC and TOM in coastal sediments was suggested in this study. The new method may reduce the number of required samples (stations) and calculation time, and associated expenses based on structural sampling methods.

This method calculates effective weight for horizontal and vertical distances separately based on transfer and carrying media. Unlike the kriging method, this approach varies in its power for the distance between stations. Additionally, it considers all stations and considers the effect of water wave direction when considering nearby stations. The calculation pattern was illustrated in Figs. 2 and 3. indicating four scenarios. In the neighborhood scenario (C_I), the mean concentration (i.e., C_{mean}) is determined by computing the average concentration from the surrounding stations (Fig. 2a). Likewise, for the sea-to-coast (C_{II}) and coast-to-sea (C_{III}) scenarios, C_{mean} is computed using measurements solely from the surrounding stations on the sea (Fig. 2b) and coast side (Fig. 2c), respectively. Lastly, the total scenario (C_{IV}) utilizes all available stations (Fig. 2d), including the substation under analysis, to calculate C_{mean}.

As shown in Fig. 3, different weights (Eq. (1)) for horizontal and vertical distance on the surface local coordination system were applied.

$$W_i = \left(f_y \times (Y_i - y_0)^2 + f_x \times (X_i - X_0)^2\right)^{0.5} \quad (1)$$

Y_0: coordination of the station that the concentration which obtain by formula in horizontal direction.
X_0: coordination of the station that the concentration which obtain by formula in vertical direction.
Y_i: coordination of the stations that the concentration is given in horizontal direction.
X_i: coordination of the stations that the concentration is given in vertical direction.
W_i: distance between the station that concentration is given and the station that concentration is estimating.

Various routes were used to estimate TOC and TOM concentration, considering the effects of distance (power Wi), mean concentration of effective stations and direction of probable transfer have been shown in Fig. 3. The verification of C_{mean} scenarios and the impact of neighboring stations on topology are crucial to identifying the origin of detected hydrocarbons. This analysis will clarify the direction of hydrocarbon transfer within intertidal coastal sediment, allowing for a better understanding of the transferal orientation of these substances. Therefore, it will be possible to confirm whether hydrocarbons come from terrestrial or marine sources and evaluate the effectiveness of new estimation models. After C_{mean} calculation for each station and determining the distance between the stations using various f_x and f_y values, the concentration at each station can be estimated using Eq. (2).

$$C_{estimated} = \sum \left(\frac{C_i}{W_i^P}\right) \times C_{mean} \quad (2)$$

where C_i is the concentration of the station that distance between this station and the station which concentrate is estimating.

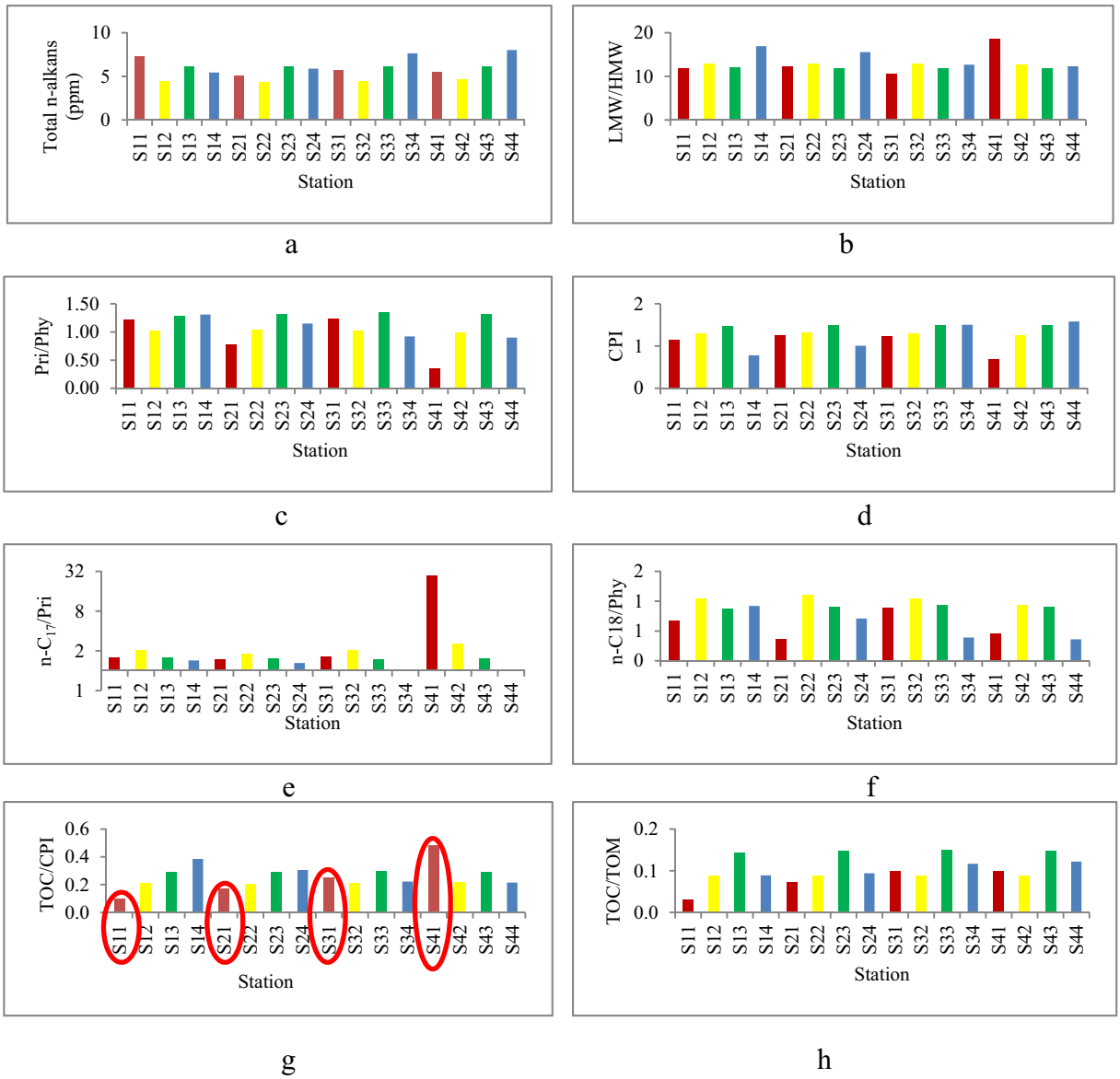

Fig. 4. Bar charts of row data of hydrocarbon pollution indices; a) Total n-alkanes, b) LMW/HMW index, c) Pri/Phy index, d) CPI index, e) n-C_{17}/Pri, f) n-C_{18}/Phy, g) TOC/CPI bar chart, h) TOC/TOM bar chart.

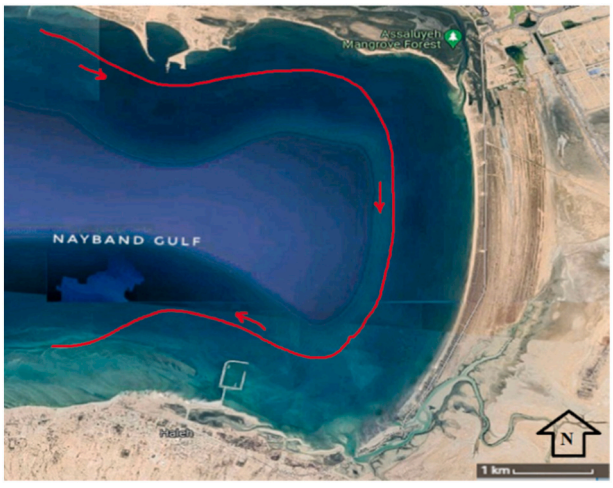

Fig. 5. Gulf Stream flow in sampling site.

3. Results and discussion

The C_{mean} results obtained using the proposed geostatistical estimation method were summarized in Tables 1 and 2, which present the values for TOC and TOM, respectively. The associated evaluation results were also tabulated in Tables 3, 4 and 5.

The concentration of total n-alkanes in the sediment ranged from 4.29 to 8.02 μg/g (Table 6). n-Alkanes concentration <10 μg/g considered as unpolluted area (Volkman, 1986). According to Fig. 4a, the total amount of normal alkanes in 80 % of stations was observed at around 6 ppm. The highest amount appeared at station S_{44} which is located close to the inter-city road in the east. The lowest concentration found was 4.29 ppm at station S_{22}.

The ratio of LMW/HMW ranged from 12.32 to 18.56 (Table 6). For the LMW/HMW index, 80 % of the stations showed a value of <15, the highest ratio was found at station S_{41} near the Mangrove plants, and the lowest ratio was observed at station S_{31} (Fig. 4b). Ratios less than one (≪1), indicate the origin of vascular plants, around one (~1), indicate oil or plankton sources and the high ratios of this index(≫1), indicate fresh oil content (Kucuksezgin et al., 2012; Xuelu Gaoa, 2008). So, the

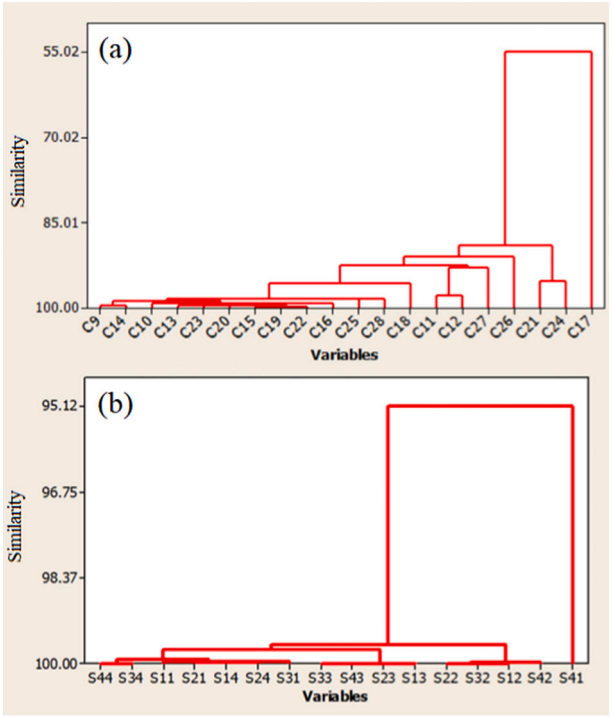

Fig. 6. Dendrogram of cluster analysis of a) n-alkanes and (b) stations for all variables.

results of LMW/HMW showed the main sources of hydrocarbons are fresh oil and gas condensate.

The Pri/Phy ratio near 1 (~1) indicates petrogenic sources (Commendatore and Esteves, 2004; Ou et al., 2004). The Pri/Phy index of about 50 % of the station had a value of close to one, the highest value for this indicator was found at station S_{33} while the lowest occurred at station S_{41} (Fig. 4c). Overall, the ratio ranged from 0.36 to 1.34 (Table 6). This range demonstrates petrogenic sources. So biogenic origin of hydrocarbons (Mille et al., 2007) could be a weak suggestion.

CPI value was found in the range from 0.69 to 1.58 as shown in Table 6. For most stations the CPI value is greater than one and <2, the highest was obtained at station S_{44} and the lowest at station S_{41} (Fig. 4d). CPI values which are close to one (~1), indicate human sources such as oil pollution, whereas values larger than 3 (≫3), have to be considered as an evidence for natural sources (Gomes and Azevedo, 2003; Ou et al., 2004). Here in this study, results figured out the human sources of hydrocarbons.

The ratios of n-C_{17}/Pri and n-C_{18}/Phy ranged from 0.99 to 27.78 and 0.36 to 1.11, respectively, as is shown in Table 6. Values <2 (≪2), indicate the presence of degraded oil while values greater or equal to 2, suggest recent oil production (Colombo et al., 1989; Díez et al., 2007; Ezra et al., 2000). For n-C_{17}/Pri, 70 % of stations were <2 and the highest value was found at S_{41} (Fig. 4e). In all stations, n-C_{18}/Phy index values were <2 (Fig. 4f). These indices declared degraded oil (Maciel et al., 2016) for most of stations while individual station of S_{41} where is located in mangroves' forest zone seems support recent oil production as a suggestion. Station S_{41} is extremely higher than other stations for n-C_{17}/Pri, which may lead new attention to investigation of different response of sediments in salt marshes anomaly.

Coupling the extracted data of LMW/HMW and n-C_{17}/Pri may drive the research toward the augmentation of the hypothesis on low oxidation and low degradation of hydrocarbons in salt marshes and mangroves forests. Thus, a possible explanation for the high amount of LMW/HMW at S_{41} could be wetland swamp which covers the surface sediment with saline dense water and protected it from atmosphere contact and quick natural oxidation/degradation (Pu et al., 2017). Wetlands also decrease the temperature in its bottom sediment dramatically compared with surface sediment, outside of mangrove forest.

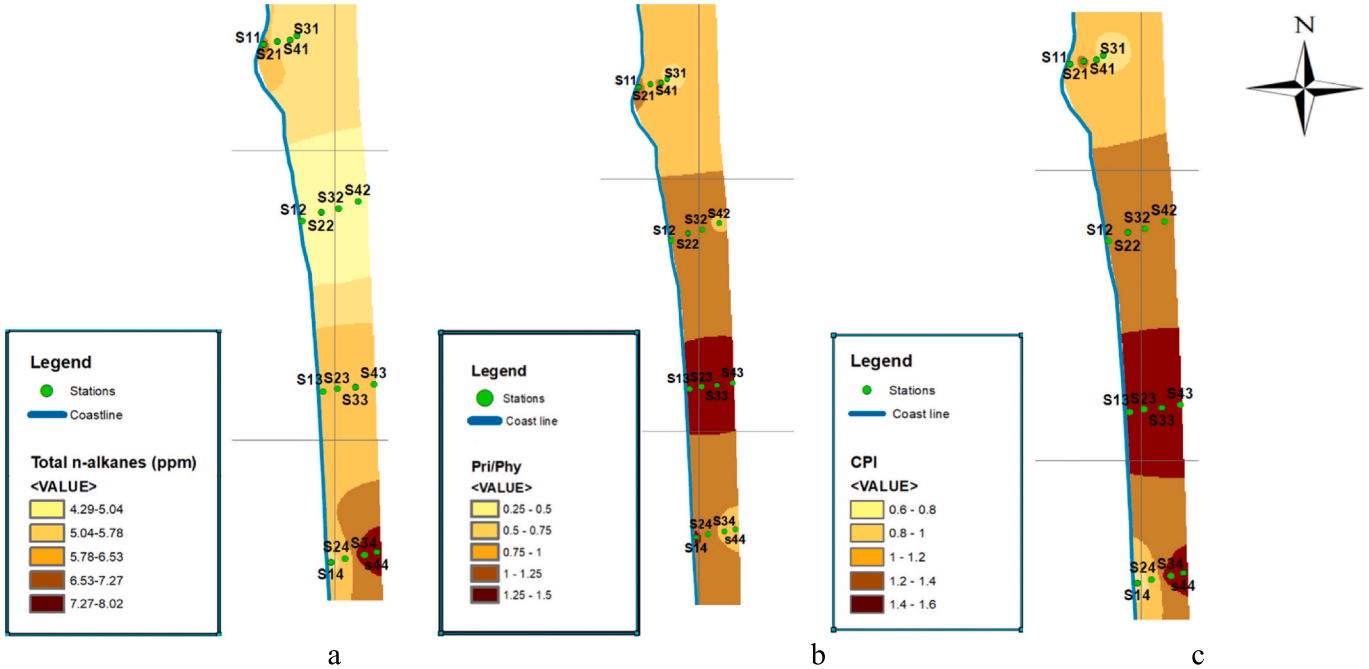

$$a)\,Total\ n\text{-}alk_{i,j}=\begin{bmatrix}7329.47 & 4412.77 & 6134.35 & 5445.69\\ 5078.99 & 4294.12 & 6150.13 & 5881.19\\ 5659.11 & 4387.95 & 6158.52 & 7649.66\\ 5504.83 & 4637.53 & 6150.23 & 8024.97\end{bmatrix}\quad b)\,\frac{Pri}{Phy}\,index_{i,j}=\begin{bmatrix}1.22 & 1.02 & 1.28 & 1.31\\ 0.78 & 1.03 & 1.32 & 1.15\\ 1.24 & 1.02 & 1.34 & 0.92\\ 0.36 & 0.99 & 1.32 & 0.90\end{bmatrix}\quad c)\,CPI\ index_{i,j}=\begin{bmatrix}1.14 & 1.29 & 1.47 & 0.78\\ 1.25 & 1.32 & 1.49 & 1.01\\ 1.23 & 1.30 & 1.50 & 1.51\\ 0.69 & 1.26 & 1.49 & 1.58\end{bmatrix}$$

Fig. 7. Zoning map via geostatistical analysis of aliphatic hydrocarbons indices; a) Total n-alkans, b) Pri/Phy index, c) CPI index.

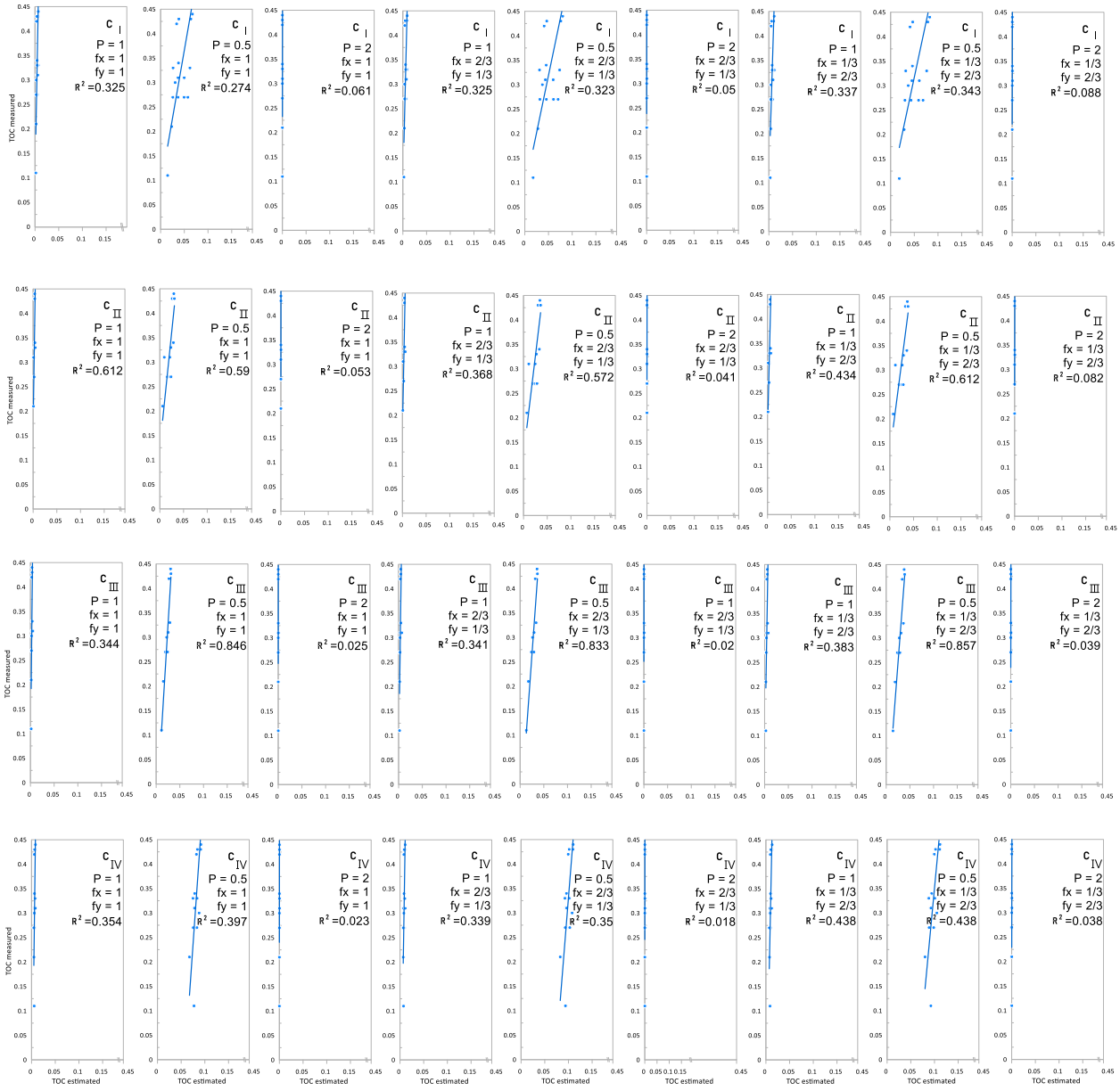

Fig. 8. Estimation values of TOC vs. measured values.

As mentioned, the LMW/HMW and n-C_{17}/Pri are issuing the hypothesis of impacts from fresh oil. The role of mangroves' species in adsorption of hydrocarbons from water (Cheque et al., 2017; Partani et al., 2015) and sediments (Brito et al., 2006; Hoff, 2002) is another issue that may describe low concentration of hydrocarbons in station S_{41} where is located in salt marsh and mangrove area. Land plants contribution as a autochthonous hydrocarbon source is not acceptable according to lower contents of n-C_{29} (Mille et al., 2007). So, a mixture of hydrocarbons referring to degraded oil and fresh oil were detected in most of the stations while the human activities are the basis of the n-alkanes.

The concentration of n-alkanes exhibits a predominant ascending spatial trend along the coastline toward the southern direction. However, this contradicts the expected Nayband Bay flow, which is known to be clockwise (Yao and Johns, 2010) (Fig. 5). Given that the sampling site was smaller than the effective scale of the large marine sediment transport controlled by the bay flow, any consequences of the bay flow would likely affect all stations with similar levels of effect. To confirm this suggestion and enhance the topological resolution of hydrocarbon monitoring with minimum station monitoring, we have employed inter-estimation methods using neighborhood stations to develop a new quick estimation method. This approach will be further refined by effective C_{mean} scenarios. It is plausible that local hydraulic characteristics due to the morphology of the bay, such as secondary currents, could be the primary carrier of hydrocarbons.

The ratio of TOC/CPI increases toward terrestrial area on the northern transect (stations S_{11} to S_{14}). The trend of TOC/CPI approves the role of mangroves and salt marshes in hydrocarbon concentration where the organic carbons (TOC) are increasing as indicators of organic matter source (Zhang et al., 2018). On the other hand, <12 % of TOM is TOC and the relation of TOC/TOM is approximately constant (ranged from 0.03 to 0.14) that is addressing lower contribution of organic carbons and natural hydrocarbons in sediment (Fig. 4.h). So human activity is identified as the main source of hydrocarbons.

The PPCA coefficients between n-alkanes measured at the sample sites were calculated. According to these calculations, it was found that >50 % of the n-alkanes had same correlation coefficient (>0.9 for R^2) as well as for stations were observed >90 %. It means there is no significant

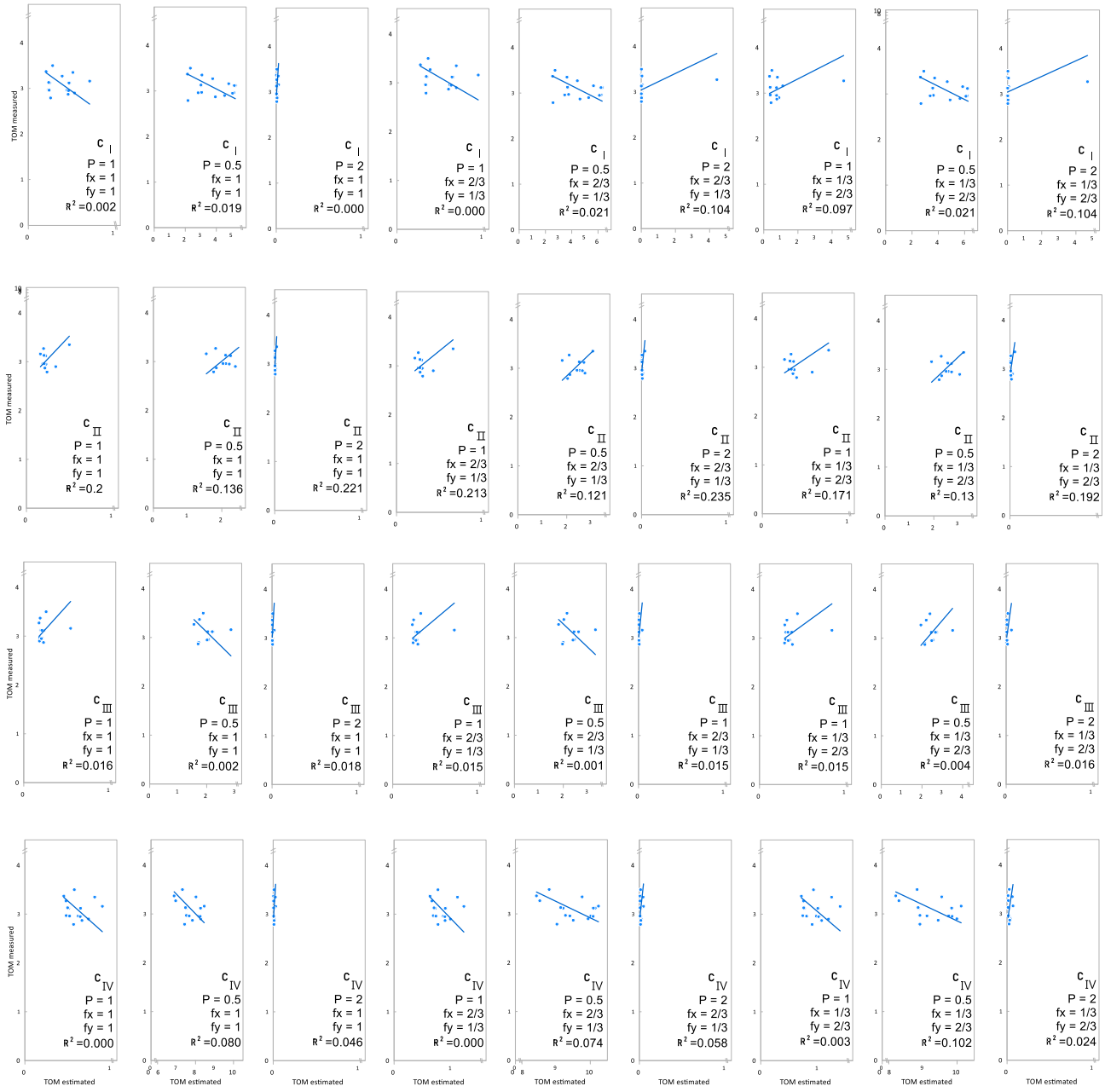

Fig. 9. Estimation values of TOM vs. measured values.

variation between stations for n-alkanes and it could explain the exotic effective factors from outside of the boundaries of study site. The PPCA revealed >90 % of Pearson correlation number for C_{16} and C_9, C_{15} and C_{10}, C_{22} with C_{19} and C_{20}, C_{25} with C_{15} and C_{19} and C_{20} etc. Correlation observations between LMW and HMW show that there may be some correlation between hydrocarbons such as C_{25} with C_9 to C_{16}, C_{28} with C_{10} to C_{15}, C_{22} and C_{23} with C_9 to C_{16}.

Cluster analysis confirmed the outcomes of PPCA. A high similarity[1] between clusters in station analysis could be found for all hydrocarbons. However, minor variation along the coastline should have been investigated more carefully. Station S_{41}, exhibits individual features and thus it has been put into an independent cluster (Fig. 6b). Cluster analysis results between stations (Fig. 6b) forms two major clusters while station S_{41} stands as an individual cluster and all clusters showed up with similarity of 95 % and greater. Similarity of 85 % and greater in all hydrocarbons observed in cluster analysis in stations and C_{21}, C_{17} and C_{24}. C_{17} which are a key variable that introduced with Pri. (Fig. 6a) have less similarity value.

Applying Geo-spatial zoning indicated that the total amount of n-alkanes decreased by moving northwards and increased with reaching the Mangrove plants (S_{41} is in mangroves forest). Also, the highest concentrations were observed near the road in the east (Fig. 7a). For the Pri/Phy index, the values of this index decreased by moving northward (along the coastline) (Fig. 7b). For the CPI, the index was reduced moving in the direction toward the north. The CPI index approved the human activities in two closest stations (S_{34}, S_{44}) to **intercity road** (Fig. 7c). This phenomenon would be explained by vehicle traffic and fuel consumption and hydrocarbon emission that may wash up by run-

[1] Similarity in cluster analysis expresses the smaller internal distance of members of each cluster in final hierarchical cluster analysis. If the members of each cluster moved to another one the sum of internal distance between members of new clusters would be greater and similarity will decrease.

Table 9
Same as Table 8 but for TOC.

MCS	P	fx	fy	R2	RMSE	RSS	TSS	VAR_U	B1po	B1op	RSR
Coast to Sea	0.50	0.33	0.67	0.004	0.76	7.0	0.417	0.146	2.050	0.488	0.58
		0.67	0.33	0.001	0.87	9.2	0.417	0.153	7.023	0.142	0.77
		1.00	1.00	0.002	1.17	16.4	0.417	0.106	1.524	0.656	1.37
	1.00	0.33	0.67	0.015	2.73	89.7	0.417	0.021	0.784	1.275	7.48
		0.67	0.33	0.015	2.81	94.5	0.417	0.016	0.680	1.470	7.88
		1.00	1.00	0.016	2.88	99.4	0.417	0.009	0.005	194.820	8.29
	2.00	0.33	0.67	0.016	3.10	115.3	0.417	0.000	0.079	12.638	9.61
		0.67	0.33	0.020	3.11	115.7	0.417	0.000	0.052	19.310	9.65
		1.00	1.00	0.018	3.11	116.0	0.417	0.000	0.033	30.163	9.67
Sea to Coast	0.50	0.33	0.67	0.130	0.60	4.3	0.315	0.118	2.119	0.472	0.36
		0.67	0.33	0.121	0.70	5.9	0.315	0.115	8.081	0.124	0.49
		1.00	1.00	0.136	1.02	12.5	0.315	0.081	1.754	0.570	1.04
	1.00	0.33	0.67	0.171	2.66	84.8	0.315	0.019	0.843	1.186	7.07
		0.67	0.33	0.213	2.73	89.7	0.315	0.013	0.705	1.419	7.47
		1.00	1.00	0.200	2.81	94.6	0.315	0.008	0.541	1.848	7.88
	2.00	0.33	0.67	0.192	3.04	110.7	0.315	0.000	0.084	11.883	9.22
		0.67	0.33	0.235	3.04	111.1	0.315	0.000	0.060	16.783	9.26
		1.00	1.00	0.221	3.05	111.4	0.315	0.000	0.035	28.703	9.28
Neighborhoods	0.50	0.33	0.67	0.021	1.98	62.8	0.597	1.787	6.918	0.145	3.93
		0.67	0.33	0.021	1.93	59.8	0.597	1.755	6.995	0.143	3.73
		1.00	1.00	0.019	1.32	27.8	0.597	1.215	9.632	0.104	1.74
	1.00	0.33	0.67	0.097	2.43	94.8	0.597	1.017	5.219	0.192	5.92
		0.67	0.33	0.000	2.60	108.0	0.597	0.036	5.111	1.020	6.75
		1.00	1.00	0.002	2.72	118.2	0.597	0.021	1.065	0.939	7.39
	2.00	0.33	0.67	0.104	2.99	143.2	0.597	1.270	5.833	0.171	8.95
		0.67	0.33	0.104	2.99	143.3	0.597	1.141	5.527	0.181	8.96
		1.00	1.00	0.000	3.09	153.1	0.597	0.000	0.036	28.052	9.57
Total	0.50	0.33	0.33	0.67	0.102	6.22	618.3	0.597	0.341	3.023	0.331
		0.67	0.67	0.33	0.074	6.41	657.7	0.597	0.330	6.856	0.146
		1.00	1.00	1.00	0.080	4.71	354.5	0.597	0.233	2.499	0.400
	1.00	0.33	0.33	0.67	0.003	2.16	74.8	0.597	0.038	1.003	0.997
		0.67	0.67	0.33	0.000	2.27	82.4	0.597	0.026	0.664	1.506
		1.00	1.00	1.00	0.000	2.49	99.5	0.597	0.015	0.005	199.560
	2.00	0.33	0.33	0.67	0.024	3.08	151.4	0.597	0.000	0.087	11.551
		0.67	0.67	0.33	0.058	3.09	152.4	0.597	0.000	0.051	19.780
		1.00	1.00	1.00	0.046	3.09	153.0	0.597	0.000	0.036	27.747

off. Therefore, they may be affected by oil and gas industries despite having no interface in boundaries and the distance. A lower amount than average of measured concentration of hydrocarbons (Fig. 7a) and less value of CPI and Pri/Phy (Fig. 7b, c) support the idea of the role mangroves in hydrocarbon adsorption.

The homogeneity of physical properties in particles avoids embedding any relation between the hydrocarbon's indices and particles size. In terms of particle size and hydrocarbons, no evidence have been found about the size impacts on the hydrocarbons adsorption (Maciel et al., 2016) in the study area.

3.1. Results for inter-estimation calculations

Considering C_{mean} values calculated for each station (see Table 1) and the distance between each station (see Tables 3, 4, and 5), the concentration at each station was estimated and depicted in Figs. 8 and 9. In most cases, the estimated amount falls below the actual amount in the graphs. Furthermore, the trend of the estimated graphs shows a positive linear slope when compared to the measurements. Notably, the coast-to-sea scenario exhibits the highest linear correlation coefficient, while the neighborhoods scenario has the lowest coefficient (Fig. 8).

In the study, a range of statistical indicators were employed to evaluate the effectiveness of the proposed methods and compare the predicted and measured concentrations. The Root Mean Squared Error (RMSE) was used to measure the accuracy of predictions, which calculates the squared difference between predicted and actual values. This widely-used indicator is particularly useful for comparing forecasting errors across different models or configurations of a variable (Christie and Neill, 2022).

To determine the amount of variance that can be explained by a particular model or factor, the Total Sum of Squares (TSS) was used. This indicator is calculated as the sum of the squared differences between each observation and the mean of all the observations. TSS can help estimate the amount of explained variance and serves as a benchmark for evaluating model performance (Mohr et al., 2022).

B1, an important statistic for describing bivariate scatter that is obtained from SMA regression and is invariant to axis orientation, was also employed. B1 was used to test the isometry of PO[2] scatter and represents the ratio of standard deviations. (Warton et al., 2006). To combine the statistics of the error index and a normalization factor, the Relative Squared Error (RSR) was used. This index varies between 0 and 1, with values closer to zero indicating a more accurate model simulation (Moriasi et al., 2007).

Finally, the Percent Mean Squared Error (PLA) was used to evaluate the accuracy of the estimated concentrations. This measure determines the percentage of MSE associated with systematic differences in predictions. By using these statistical indicators, the researchers were able to thoroughly evaluate the proposed methods and compare the predicted and measured concentrations (Correndo et al., 2021).

The ternary chart displays (Fig. 10) how the correlation coefficient (R^2) varies with changes in the parameters f_x, f_y, and P. The figure clearly indicates that the highest R^2 value was observed at low P values ($P < 0.05$).

The reliability of the topological correlation method for determining the parameter of organic compounds is questionable. Thus, relying on statistical methods to develop an equation for enhancing the resolution of organic compounds may not be effective. Instead, to confirm the origin of identified organic carbon and estimate this parameter in

[2] The ratio of standard deviations predicted and observed values.

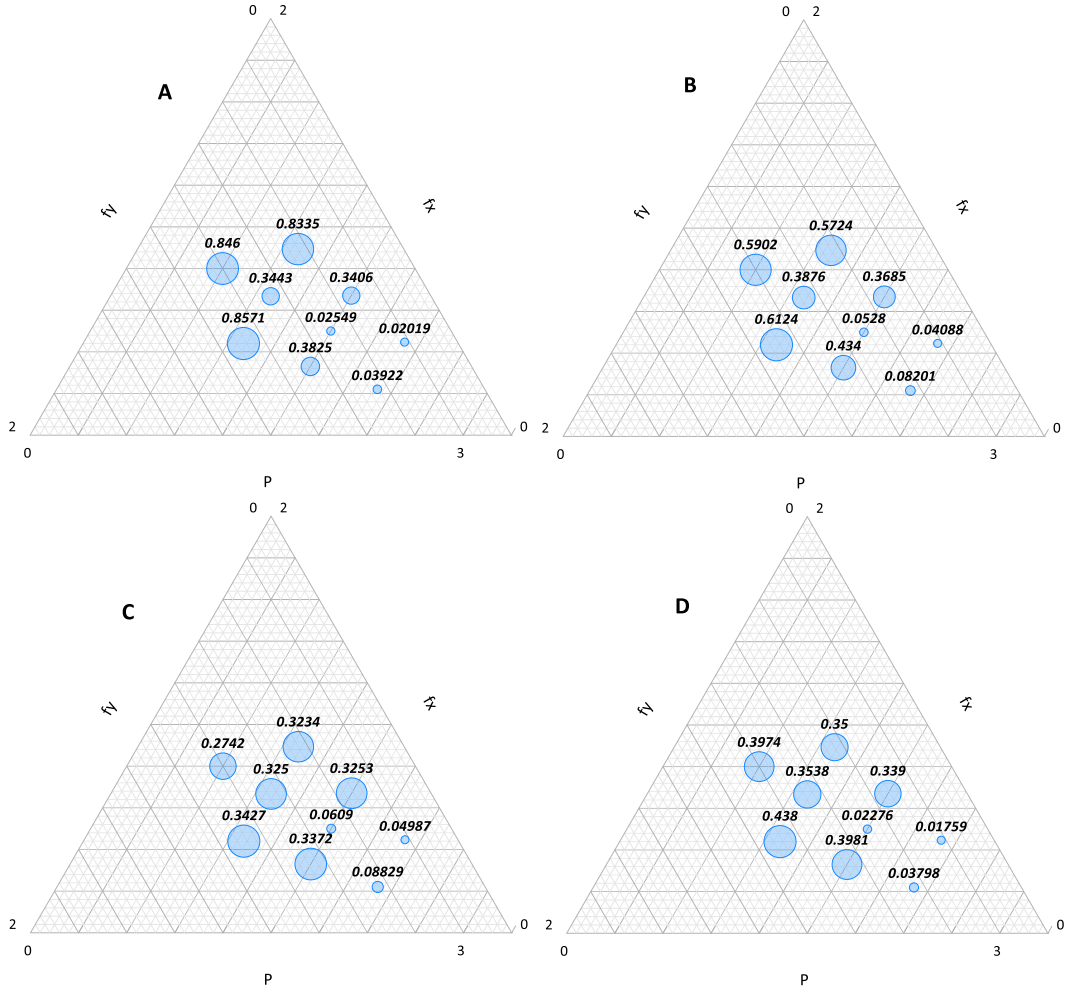

Fig. 10. Scatter correlation coefficient (R^2): a) Coast to Sea (C_{III}) b) Sea to Coast (C_{II}) c) Neighborhoods (C_I) d) Total (C_{IV}) for TOC.

Table 11
Stratification of mean concentration scenarios based on statistical indicators.

MCS	P	fx	fy	R2	RMSE	RSS	VAR_U	RSR	Total point	Level
Coast to Sea	0.50	0.33	0.67	3	1	3	2	3	12	A
		0.67	0.33	3	1	3	2	3	12	A
		1.00	1.00	3	1	3	2	3	12	A
	1.00	0.33	0.67	1	2	2	3	3	11	B
Sea to Coast	0.50	0.33	0.67	2	1	2	2	3	10	B
		0.67	0.33	2	1	2	2	3	10	B
		1.00	1.00	2	1	2	3	2	10	B
	1.00	0.33	0.67	1	1	2	3	2	9	C
Neighborhoods	0.50	0.33	0.67	1	2	2	1	3	9	C
		0.67	0.33	1	2	2	1	3	9	C
		1.00	1.00	1	2	2	1	3	9	C
	1.00	0.33	0.67	1	1	1	3	2	8	C
Total	0.50	0.33	0.67	1	3	3	2	3	12	A
		0.67	0.33	1	3	3	2	3	12	A
		1.00	1.00	1	3	3	2	3	12	A
	1.00	0.33	0.67	1	1	1	3	2	8	C

petrogenic and human source layers of the same sediments, the convergence of results from equations derived from scenarios of various factors affecting the transfer of hydrocarbons is utilized. This approach ensures greater accuracy and reliability in determining the origin and quantity of organic compounds in sediment samples (Tables 9 and 10).

Initially, the states with the highest correlation coefficients were identified among each of the mean concentration scenarios. Subsequently, each statistical index was assigned a score ranging from 1 to 3. Finally, based on the cumulative scores across three levels, the states were then categorized (Table 11).

Table 10
Scoring the values of statistical indicators.

Point	R^2	RMSE	RSS	VAR_U	RSR
1	Less than 0.5	0.23_.0.26	1.4_1.7	E−5_E−4	More than 0.15
2	0.5_0.8	0.26_0.29	1.1_1.4	E−7_E−6	0.1_0.15
3	0.8_1	0.29_0.33	Less than 1.1	E−9_E−8	Less than 0.1

The average concentration scenarios were classified into three levels, and the level A scenarios were identified as the optimal functions for estimating TOC concentration values in stations where measurements are not conducted:

$$1)\ C_{III}\ C_{estimated}=\sum\left(\frac{C_i}{W_i^{0.5}}\right)\times C_{mean}\ W_i=\left(\frac{2}{3}\times\left(Y_i-y_o\right)^2+\frac{1}{3}\times\left(X_i-X_o\right)^2\right)^{0.5}$$

$$2)\ C_{III}\ C_{estimated}=\sum\left(\frac{C_i}{W_i^{0.5}}\right)\times C_{mean}\ W_i=\left(\frac{1}{3}\times\left(Y_i-y_o\right)^2+\frac{2}{3}\times\left(X_i-X_o\right)^2\right)^{0.5}$$

$$3)\ C_{III}\ C_{estimated}=\sum\left(\frac{C_i}{W_i^{0.5}}\right)\times C_{mean}\ W_i=\left(1\times\left(Y_i-y_o\right)^2+1\times\left(X_i-X_o\right)^2\right)^{0.5}$$

$$4)\ C_{IV}\ C_{estimated}=\sum\left(\frac{C_i}{W_i^{0.5}}\right)\times C_{mean}\ W_i=\left(\frac{2}{3}\times\left(Y_i-y_o\right)^2+\frac{1}{3}\times\left(X_i-X_o\right)^2\right)^{0.5}$$

$$5)\ C_{IV}\ C_{estimated}=\sum\left(\frac{C_i}{W_i^{0.5}}\right)\times C_{mean}\ W_i=\left(\frac{1}{3}\times\left(Y_i-y_o\right)^2+\frac{2}{3}\times\left(X_i-X_o\right)^2\right)^{0.5}$$

$$6)\ C_{IV}\ C_{estimated}=\sum\left(\frac{C_i}{W_i^{0.5}}\right)\times C_{mean}\ W_i=\left(1\times\left(Y_i-y_o\right)^2+1\times\left(X_i-X_o\right)^2\right)^{0.5}$$

Some suggestions may release on the pollution transfer based on predominant general flow in the gulf and considering adverse flow patterns in the bay area. Although the prevailing general current in the gulf follows a counter clockwise direction it is possible that the morphometry in bay area generates adverse secondary currents So, AHCs could be transported to the bay area from off shore drilling rig and offshore gas production installation. At some sampling stations, higher concentration in hydrocarbons were detected in lighter ones. I these cases heavy metal analysis revealed no signal of crude oil pollution according to non-detection of Vanadium and Nickel (heavy metal analysis also was carried out for eight of sampling stations) as an crude oil indicator (Ahmed, 2010). Though the oil pollution sources hypothesis of natural crude oil changed by anthropogenic and gas sources. Mangroves' zones may absorb a significant number of hydrocarbons.

4. Conclusions

The aim of this study was to identify the source of hydrocarbon pollution along the sub-tropical coastline, which hosts mangrove ecosystems near one of the largest oil and gas industries. Relevant indices were investigated, and initial suggestions for the origin of AHCs were developed. Novel topological inter-estimation measures were then employed to increase monitoring resolution and estimate missing data. The direction of probable AHCs' transmission was considered in the estimation equations, and after validation/calibration, the initial suggestions of sources were approved.

The results indicated that human activities affect hydrocarbon concentrations in sediments, despite the study area being located 11 km away from refinery sites. The refinery and industrial sites could have devastating effects on the ecosystem of the area, including the mangrove forests, leading to the disappearance of mangrove plants in the bay area and forcing mangroves to migrate toward terrestrial areas.

This research emphasized the role of study site scale on hydrocarbon dynamics in coastal sediments. The results confirmed the role of mangrove communication and salt marsh saline water on hydrocarbon adsorption via sediments. The time that has passed since industries spread to the area is too long, especially in developing countries where effective parameters in the neighboring environment cannot vary significantly. Nevertheless, the accumulation of new field study analyses and applicable knowledge on other similar study areas in different scales will provide comparative scientific consequences enriching future scientific observations.

The research pointed out that LMW values were significantly higher than HMW, confirming anthropogenic sources with gas condensate industries. The expectation of less value due to the volatilization characteristics of LMW components could not be supported by the scientific outcomes in the study area. Furthermore, while there were slight spatial variations in AHCs and indices in the study area, it could be concluded that these variations might follow the natural behavior of indices in all sampling stations. The authors believe that further research over a larger area will improve the current knowledge of the transport processes and deposition of pollutants originating from different sources, particularly those of the oil and gas industrial zone along the coastline.

Funding

This study was partly done at Antalya Bilim University under the scholarship number of 20IR008182 which had been awarded to Sadegh Partani.

CRediT authorship contribution statement

Sadegh Partani: Conceptualization, Methodology, Supervision, and Project administration; Ali Danandeh Mehr: Writing, Review and Editing; Mohsen Maghrebi: Visualization; Rouzbeh Mokhtari: Writing - Original Draft & Editing; Hans-Peter Nachtnebel: Review and Data Curation; Ricardo Hideo Taniwaki: Review; Amin Arzhangi: Formatting, Data Curation, Review and Editing.

Declaration of competing interest

The authors declare that they have no known competing financial interests or personal relationships that could have appeared to influence the work reported in this paper.

Data availability

Data will be made available on request.

Acknowledgements

We would like to thank Seyyed Hadi Abtahi, from Kargosha Research Group of Urban Human Ecology, for his assistance in organizing and categorizing the primary draft of this article.

Appendix A. Supplementary data

Supplementary data to this article can be found online at https://doi.org/10.1016/j.scitotenv.2023.166746.

References

Abbasnejadfard, M., Bastami, M., Fallah, A., 2021. Investigating the spatial correlations in univariate random fields of peak ground velocity and peak ground displacement considering anisotropy. Geoenviron. Disasters 8 (1), 24. https://doi.org/10.1186/s40677-021-00196-w.

Ahmed, T., 2010. Reservoir Engineering Handbook. Gulf Professional Publishing. https://doi.org/10.1016/B978-1-85617-803-7.50009-2.

Akhbarizadeh, R., Moore, F., Keshavarzi, B., Moeinpour, A., 2016. Aliphatic and polycyclic aromatic hydrocarbons risk assessment in coastal water and sediments of Khark Island, SW Iran. Mar. Pollut. Bull.

Alizadeh, B., Maroufi, K., Fajrak, M., 2018. Oil-oil correlation, geochemical characteristics, and origin of hydrocarbons from Mansourabad oilfield, SW Iran. J. Afr. Earth Sci. 147 (December 2016), 383–392. https://doi.org/10.1016/j.jafrearsci.2018.06.008.

Ashournejad, Q., Amiraslani, F., Moghadam, M.K., Toomanian, A., 2019. Assessing the changes of mangrove ecosystem services value in the Pars Special Economic Energy Zone. Ocean Coast. Manag. 179 (May), 104838 https://doi.org/10.1016/j.ocecoaman.2019.104838.

Balgobin, A., Ramroop Singh, N., 2019. Source apportionment and seasonal cancer risk of polycyclic aromatic hydrocarbons of sediments in a multi-use coastal environment containing a Ramsar wetland, for a Caribbean island. Sci. Total Environ. 664, 474–486. https://doi.org/10.1016/j.scitotenv.2019.02.031.

Brink, H.J., 2022. Albert Einstein, world of dices and hydrocarbon system analysis. Int. J. Sustain. Energy Environ. Res. 11 (2), 86–103. https://doi.org/10.18488/13.v11i2.3154.

Brito, E.M.S., Guyoneaud, R., Goñi-Urriza, M., Ranchou-Peyruse, A., Verbaere, A., Crapez, M.A.C., Wasserman, J.C.A., Duran, R., 2006. Characterization of hydrocarbonoclastic bacterial communities from mangrove sediments in Guanabara Bay, Brazil. Res. Microbiol. 157 (8), 752–762. https://doi.org/10.1016/j.resmic.2006.03.005.

Cheque, L., Pires, J., Coelho, C., Sabadini, E., Castillo, D., Alves, R., Araujo, M., Crapez, C., 2017. Response of mangrove propagules to the presence of oil and hydrocarbon degrading bacteria during an experimental oil spill. Lat. Am. J. Aquat. Res. 45 (4), 814–821. https://doi.org/10.3856/vol45-issue4-fulltext-17.

Christie, D., Neill, S.P., 2022. 8.09—Measuring and observing the ocean renewable energy resource. In: Letcher, T.M. (Ed.), Comprehensive Renewable Energy, second edition. Elsevier, pp. 149–175. https://doi.org/10.1016/B978-0-12-819727-1.00083-2.

Colombo, J.C., Pelletier, E., Brochu, C., Khalil, M., Catoggio, J.A., 1989. Determination of hydrocarbon sources using n-alkane and polyaromatic hydrocarbon distribution indexes. Case study: Rio de la Plata Estuary, Argentina. Environ. Sci. Technol. 23 (7), 888–894. https://doi.org/10.1021/es00065a019.

Commendatore, M.G., Esteves, J.L., 2004. Natural and anthropogenic hydrocarbons in sediments from the Chubut River (Patagonia, Argentina). Mar. Pollut. Bull. 48 (9–10), 910–918. https://doi.org/10.1016/j.marpolbul.2003.11.015.

Commendatore, M.G., Nievas, M.L., Amin, O., Esteves, J.L., 2012. Sources and distribution of aliphatic and polyaromatic hydrocarbons in coastal sediments from the Ushuaia Bay (Tierra del Fuego, Patagonia, Argentina). Mar. Environ. Res. 74, 20–31. https://doi.org/10.1016/j.marenvres.2011.11.010.

Correndo, A.A., Hefley, T.J., Holzworth, D.P., Ciampitti, I.A., 2021. Revisiting linear regression to test agreement in continuous predicted-observed datasets. Agric. Syst. 192, 103194 https://doi.org/10.1016/j.agsy.2021.103194.

Dai, Z., Ma, Z., Zhang, X., Chen, J., Ershadnia, R., Luan, X., Soltanian, M.R., 2022. An integrated experimental design framework for optimizing solute transport monitoring locations in heterogeneous sedimentary media. J. Hydrol. 614, 128541.

Dashtbozorg, M., Riyahi Bakhtiari, A., Shushizadeh, M.R., Taghavi, L., 2019. Quantitative evaluation of n-alkanes, PAHs, and petroleum biomarker accumulation in beach-stranded tar balls and coastal surface sediments in the Bushehr Province, Persian Gulf (Iran). Mar. Pollut. Bull. 146 (July), 801–815. https://doi.org/10.1016/j.marpolbul.2019.07.023.

Davari, A., Danehkar, A., Khorasani, N., Javanshir, A., 2010. An investigation on accumulation of heavy metals in roots and leaves of *Avicennia marina* the sediment, Bushehr, the Persian Gulf. J. Nat. Environ. 63 (3), 267–277.

Davoodi, H., Gharibreza, M., Negarestan, H., Mortazavi, M.S., Lak, R., 2017. Ecological risk assessment of the Assaluyeh and Bassatin estuaries (northern Persian Gulf) using sediment quality indices. Estuar. Coast. Shelf Sci. 192, 17–28. https://doi.org/10.1016/j.ecss.2017.05.003.

de Arruda-Santos, R.H., Schettini, C.A.F., Yogui, G.T., Maciel, D.C., Zanardi-Lamardo, E., 2018. Sources and distribution of aromatic hydrocarbons in a tropical marine protected area estuary under influence of sugarcane cultivation. Sci. Total Environ. 624, 935–944. https://doi.org/10.1016/j.scitotenv.2017.12.174.

Díez, S., Jover, E., Bayona, J.M., Albaigés, J., 2007. Prestige oil spill. III. Fate of heavy oil in the marine environment. Environ. Sci. Technol. 41 (9), 3075–3082. https://doi.org/10.1021/es0629559.

Duan, L., Song, J., Yuan, H., Li, X., Peng, Q., 2019. Occurrence and origins of biomarker aliphatic hydrocarbons and their indications in surface sediments of the East China Sea. Ecotoxicol. Environ. Saf. 167 (September 2018), 259–268. https://doi.org/10.1016/j.ecoenv.2018.10.011.

Duke, N., Kathiresan, K., Salmo III, S.G., Fernando, E.S., Peras, J.R., Sukardjo, S., Miyagi, T., Ellison, J., Koedam, N.E., Wang, Y., Primavera, J., Jin Eong, O., Wan-Hong Yong, J., Ngoc Nam, V., 2010. *Avicennia marina*. The IUCN Red List of Threatened Species, p. 8235.

Ekpo, B., Oyo-Ita, O., Wehner, H., 2005. Even-n-alkane/alkene predominances in surface sediments from the Calabar River, SE Niger Delta, Nigeria. In: Die Naturwissenschaften, vol. 92. https://doi.org/10.1007/s00114-005-0639-8.

Ezra, S., Feinstein, S., Pelly, I., Bauman, D., Miloslavsky, I., 2000. Weathering of Fuel Oil Spill on the East Mediterranean Coast, vol. 31, pp. 1733–1741.

Fang, Y.K., Wang, H.C., Fang, P.H., Liang, B., Zheng, K., Sun, Q., Wang, A.J., 2023. Life cycle assessment of integrated bioelectrochemical-constructed wetland system: environmental sustainability and economic feasibility evaluation. Resour. Conserv. Recycl. 189, 106740.

Fisher, S.C., Reilly, T.J., Jones, D.K., Benzel, W.M., Griffin, D.W., Loftin, K.A., Iwanowicz, L.R., Cohl, J.A., 2015. Standard operating procedures for collection of soil and sediment samples for the Sediment-bound Contaminant Resiliency and Response (SCoRR) strategy pilot study. In: Open-File Report. https://doi.org/10.3133/ofr20151188B.

Flemming, B.W., 2000. A revised textural classification of gravel-free muddy sediments on the basis of ternary diagrams. Cont. Shelf Res. 20 (10−11), 1125–1137. https://doi.org/10.1016/S0278-4343(00)00015-7.

Gomes, A.D.O., Azevedo, D.D.A., 2003. Aliphatic and aromatic hydrocarbons in tropical recent sediments of Campos dos Goytacazes, RJ, Brazil. J. Braz. Chem. Soc. 14 (3), 358–368. https://doi.org/10.1590/S0103-50532003000300004.

Gries, T.H., 2007. Quality Assurance Project Plan Assessment of Sediment Toxicity Quality Assurance Project Plan Assessment of Sediment Toxicity near Post Point (Bellingham Bay).

Harvey, Rodger H., Taylor, Karen A., 2017. Alkane and polycyclic aromatic hydrocarbons in sediments and benthic invertebrates of the Northern Chukchi Sea. Deep-Sea Res. II 144, 52–62. https://doi.org/10.1016/j.dsr2.2017.08.011.

Hoff, R.Z., 2002. Oil Spills in Mangroves: Planning & Response Considerations. United States. National Ocean Service. Office of Response and Restoration.

Kashif, M., Sang, Y., Mo, S., ur Rehman, S., Khan, S., Khan, M.R., Jiang, C., 2023. Deciphering the biodesulfurization pathway employing marine mangrove *Bacillus aryabhattai* strain NM1-A2 according to whole genome sequencing and transcriptome analyses. Genomics 115 (3), 110635.

Keshavarzifard, M., Moore, F., Keshavarzi, B., Sharifi, R., 2017. Distribution, source apportionment and health risk assessment of polycyclic aromatic hydrocarbons (PAHs) in intertidal sediment of Asaluyeh, Persian Gulf. In: Environmental Geochemistry and Health, vol. 40. https://doi.org/10.1007/s10653-017-0019-2.

Kucuksezgin, F., Pazi, I., Gonul, L.T., 2012. Marine organic pollutants of the Eastern Aegean: aliphatic and polycyclic aromatic hydrocarbons in Candarli Gulf surficial sediments. Mar. Pollut. Bull. 64 (11), 2569–2575. https://doi.org/10.1016/j.marpolbul.2012.07.019.

Li, W., Shi, Y., Zhu, D., Wang, W., Liu, H., Li, J., Shi, N., Ma, L., Fu, S., 2021. Fine root biomass and morphology in a temperate forest are influenced more by the nitrogen treatment approach than the rate. Ecol. Indic. 130, 108031 https://doi.org/10.1016/j.ecolind.2021.108031.

Li, R., Wu, X., Tian, H., Yu, N., Wang, C., 2022. Hybrid memetic pretrained factor analysis-based deep belief networks for transient electromagnetic inversion. IEEE Trans. Geosci. Remote Sens. 60, 1–20.

Lin, X., Lu, K., Hardison, A.K., Liu, Z., Xu, X., Gao, D., Gardner, W.S., 2021. Membrane inlet mass spectrometry method (REOX/MIMS) to measure 15N-nitrate in isotope-enrichment experiments. Ecol. Indic. 126, 107639.

Lu, Y., Meyers, P.A., 2009. Sediment lipid biomarkers as recorders of the contamination and cultural eutrophication of Lake Erie, 1909–2003. Org. Geochem. 40 (8), 912–921. https://doi.org/10.1016/j.orggeochem.2009.04.012.

Maciel, D.C., de Souza, J.R.B., Taniguchi, S., Bícego, M.C., Schettini, C.A.F., Zanardi-Lamardo, E., 2016. Hydrocarbons in sediments along a tropical estuary-shelf transition area: sources and spatial distribution. Mar. Pollut. Bull. 113 (1–2), 566–571. https://doi.org/10.1016/j.marpolbul.2016.08.048.

Madany, I.M., Jaffar, A., Al-Shirbini, E.S., 1998. Variations in the concentrations of aromatic petroleum hydrocarbons in Bahraini coastal waters during the period October 1993 to December 1995. Environ. Int. 24 (1–2), 61–66.

Mahmoodi, M., Safahieh, A., Nikpour, Y., Ghanemi, K., 2012. Distribution and sources of polycyclic aromatic hydrocarbonsin the sediment of Bushehr coastal zone-Iran. Iran. J. Energy Environ. 3 (2), 173–179. https://doi.org/10.5829/idosi.ijee.2012.03.02.0311.

Marzi, R., Torkelson, B.E., Olson, R.K., 1993. A revised carbon preference index. In: Organic Geochemistry, vol. 20. https://doi.org/10.1016/0146-6380(93)90016-5.

Mehdinia, A., Aghadadashi, V., Fumani, N.S., 2015. Origin, distribution and toxicological potential of polycyclic aromatic hydrocarbons in surface sediments from the Bushehr coast, The Persian Gulf. Mar. Pollut. Bull. 90 (1), 334–338. https://doi.org/10.1016/j.marpolbul.2014.09.021.

Mille, G., Asia, L., Guiliano, M., Malleret, L., Doumenq, P., 2007. Hydrocarbons in coastal sediments from the Mediterranean Sea (Gulf of Fos area, France) hydrocarbons in coastal sediments from the Mediterranean sea (Gulf of Fos area, France). Mar. Pollut. Bull. 54 (November 2016), 566–575. https://doi.org/10.1016/j.marpolbul.2006.12.009.

Modabberi, A., Noori, R., Madani, K., Ehsani, A.H., Mehr, A.D., Hooshyaripor, F., Kløve, B., 2020. Caspian Sea is eutrophying: the alarming message of satellite data. Environ. Res. Lett. 15 (12), 124047.

Mohebbi nozar, S.L., Ismail, W.R., Zakaria, M., 2014. Distribution, sources identification, and ecological risk of PAHs and PCBs in coastal surface sediments from the Northern Persian Gulf. In: Human and Ecological Risk Assessment, vol. 20. https://doi.org/10.1080/10807039.2014.884410.

Mohr, D.L., Wilson, W.J., Freund, R.J., 2022. Chapter 6—inferences for two or more means. In: Mohr, D.L., Wilson, W.J., Freund, R.J. (Eds.), Statistical Methods, fourth edition. Academic Press, pp. 243–299. https://doi.org/10.1016/B978-0-12-823043-5.00006-0.

Moriasi, D., G. Arnold, J., W. Van Liew, M., L. Bingner, R., D. Harmel, R., L. Veith, T., 2007. Model evaluation guidelines for systematic quantification of accuracy in watershed simulations. Trans. ASABE 50 (3), 885–900. https://doi.org/10.13031/2013.23153.

Nie, S., Mo, S., Gao, T., Yan, B., Shen, P., Kashif, M., Zhang, Z., Li, J., Jiang, C., 2023. Coupling effects of nitrate reduction and sulfur oxidation in a subtropical marine mangrove ecosystem with Spartina alterniflora invasion. Sci. Total Environ. 862, 160930 https://doi.org/10.1016/j.scitotenv.2022.160930.

Noori, R., Abbasi, M.R., Adamowski, J.F., Dehghani, M., 2017. A simple mathematical model to predict sea surface temperature over the northwest Indian Ocean. Estuar. Coast. Shelf Sci. 197, 236–243. https://doi.org/10.1016/j.ecss.2017.08.022.

Noori, R., Tian, F., Berndtsson, R., Abbasi, M.R., Naseh, M.V., Modabberi, A., Soltani, A., Kløve, B., 2019. Recent and future trends in sea surface temperature across the Persian Gulf and Gulf of Oman. PLoS One 14 (2), e0212790. https://doi.org/10.1371/journal.pone.0212790.

Ou, S., Zheng, J., Zheng, J., Richardson, B.J., Lam, P.K.S., 2004. Petroleum hydrocarbons and polycyclic aromatic hydrocarbons in the surficial sediments of Xiamen Harbour and Yuan Dan Lake, China. Chemosphere 56 (2), 107–112. https://doi.org/10.1016/j.chemosphere.2004.02.022.

Owfi, R.E., 2018. Ecological study of Harra forests in the Nayband protected area at Bushehr Province, Iran. J. Coast. Zone Manag. 21 (1), 2019. https://doi.org/10.4172/2473-3350.1000454.

Partani, Sadegh, Ghiassi, Reza, Khodadadi Darban, Ahmad, Saeedi, Mohsen, 2015. Investigating natural physical adsorption of oil content by mangroves, a field-scale study. Int. J. Environ. Res. 9 (1), 373–384.

Pu, Y., Wang, C., Meyers, P.A., 2017. Origins of biomarker aliphatic hydrocarbons in sediments of alpine Lake Ximencuo, China. Palaeogeogr. Palaeoclimatol. Palaeoecol. 475, 106–114. https://doi.org/10.1016/j.palaeo.2017.03.011.

Rastegari Mehr, M., Keshavarzi, B., Moore, F., Fooladivanda, S., Sorooshian, A., Biester, H., 2020. Spatial distribution, environmental risk and sources of heavy metals and polycyclic aromatic hydrocarbons (PAHs) in surface sediments-northwest of Persian Gulf. Cont. Shelf Res. 193, 104036 https://doi.org/10.1016/j.csr.2019.104036.

Resmi, P., Manju, M.N., Gireeshkumar, T.R., Ratheesh Kumar, C.S., Chandramohanakumar, N., 2016. Source characterisation of Sedimentary organic matter in mangrove ecosystems of northern Kerala, India: inferences from bulk characterisation and hydrocarbon biomarkers. In: Regional Studies in Marine Science, vol. 7. Elsevier Ltd. https://doi.org/10.1016/j.rsma.2016.05.006

Rossi, R.E., Dungan, J.L., Beck, L.R., 1994. Kriging in the shadows: geostatistical interpolation for remote sensing. Remote Sens. Environ. 49 (1), 32–40. https://doi.org/10.1016/0034-4257(94)90057-4.

Rostami, S., Abessi, O., Amini-Rad, H., 2019. Assessment of the toxicity, origin, biodegradation and weathering extent of petroleum hydrocarbons in surface sediments of Pars Special Economic Energy Zone, Persian Gulf. Mar. Pollut. Bull. 138 (November 2018), 302–311. https://doi.org/10.1016/j.marpolbul.2018.11.034.

Rushdi, A.I., Al-Shaikh, I., El-Mubarak, A.H., Alnaimi, H.A.J.A., Al-Shamary, N., Hassan, H.M., Abou Assali, M., 2017. Characteristics and sources of anthropogenic and biogenic hydrocarbons in sediments from the coast of Qatar. Mar. Pollut. Bull.

Sale, P.F., Feary, D.A., Burt, J.A., Bauman, A.G., Cavalcante, G.H., Drouillard, K.G., Kjerfve, B., Marquis, E., Trick, C.G., Usseglio, P., Van Lavieren, H., 2011. The growing need for sustainable ecological management of marine communities of the Persian Gulf. Ambio 40 (1), 4–17. https://doi.org/10.1007/s13280-010-0092-6.

Samsami, F., Haghshenas, S.A., Soltanpour, M., 2022. Physical and rheological characteristics of sediment for nautical depth assessment in Bushehr Port and its access channel. Water 14 (24), 24. https://doi.org/10.3390/w14244116.

Sheppard, C., Al-Husiani, M., Al-Jamali, F., Al-Yamani, F., Baldwin, R., Bishop, J., Benzoni, F., Dutrieux, E., Dulvy, N., Rao V. Durvasula, S., Jones, D.A., Loughland, R., Medio, D., Manickam, N., Pilling, G., Polikarpov, I., Price, A., Purkis, S., Riegl, B., Zainal, K., 2010. The Persian/Arabian Gulf: a young sea in decline. Mar. Pollut. Bull. 60 https://doi.org/10.1016/j.marpolbul.2009.10.017.

Soliman, Y.S., Alansari, E.M.A., Sericano, J.L., Wade, T.L., 2019. Spatio-temporal distribution and sources identifications of polycyclic aromatic hydrocarbons and their alkyl homolog in surface sediments in the central Arabian Gulf. Sci. Total Environ. 658, 787–797. https://doi.org/10.1016/j.scitotenv.2018.12.093.

Steinhauer, M.S., Boehm, P., 1992. The composition and distribution of saturated and aromatic hydrocarbons in nearshore sediments, river sediments, and coastal peat of the Alaskan Beaufort Sea: implications for detecting anthropogenic hydrocarbon inputs. In: Marine Environmental Research, vol. 33. https://doi.org/10.1016/0141-1136(92)90140-H.

Tolosa, I., de Mora, S.J., Fowler, S.W., Villeneuve, J.-P., Bartocci, J., Cattini, C., 2005. Aliphatic and aromatic hydrocarbons in marine biota and coastal sediments from the Gulf and the Gulf of Oman. Mar. Pollut. Bull. 50 (12), 1619–1633. https://doi.org/10.1016/j.marpolbul.2005.06.029.

USEPA, 1995. QA/QC Guidance for Sampling and Analysis of Sediments, Water, and Tissues for Dredged Material Evaluations Chemical Evaluations. EPA 823-B-95-001.

Usman, A.R.A., Alkredaa, R.S., Al-Wabel, M.I., 2013. Heavy metal contamination in sediments and mangroves from the coast of Red Sea: *Avicennia marina* as potential metal bioaccumulator. Ecotoxicol. Environ. Saf. 97, 263–270. https://doi.org/10.1016/j.ecoenv.2013.08.009.

Vaezzadeh, V., Zakaria, M.P., Shau-Hwai, A.T., Ibrahim, Z.Z., Mustafa, S., Abootalebi-Jahromi, F., Masood, N., Magam, S.M., Alkhadher, S.A.A., 2015. Forensic investigation of aliphatic hydrocarbons in the sediments from selected mangrove ecosystems in the west coast of Peninsular Malaysia. Mar. Pollut. Bull. 100 (1), 311–320. https://doi.org/10.1016/j.marpolbul.2015.08.034.

Volkman, J.k, 1986. Acyclic Isoprenoids as Biological Markers.

Wang, X.C., Sun, S., Ma, H.Q., Liu, Y., 2006. Sources and distribution of aliphatic and polyaromatic hydrocarbons in sediments of Jiaozhou Bay, Qingdao, China. Mar. Pollut. Bull. 52 (2), 129–138. https://doi.org/10.1016/j.marpolbul.2005.08.010.

Warton, D.I., Wright, I.J., Falster, D.S., Westoby, M., 2006. Bivariate line-fitting methods for allometry. Biol. Rev. 81 (2), 259–291. https://doi.org/10.1017/S1464793106007007.

Wei, Y., Yuanxi, L., Yu, L., Mingxiang, X., Liping, Z., Qiuliang, D., 2020. Impacts of rainfall intensity and urbanization on water environment of urban lakes. Ecohydrol. Hydrobiol. 20 (4), 513–524. https://doi.org/10.1016/j.ecohyd.2020.06.006.

Xu, Z., Wang, Y., Jiang, S., Fang, C., Liu, L., Wu, K., Chen, Y., 2022a. Impact of input, preservation and dilution on organic matter enrichment in lacustrine rift basin: a case study of lacustrine shale in Dehui Depression of Songliao Basin, NE China. Mar. Pet. Geol. 135, 105386 https://doi.org/10.1016/j.marpetgeo.2021.105386.

Xu, Z., Li, X., Li, J., Xue, Y., Jiang, S., Liu, L., Sun, Q., 2022b. Characteristics of source rocks and genetic origins of natural gas in deep formations, Gudian Depression, Songliao Basin, NE China. ACS Earth Space Chem. 6 (7), 1750–1771. https://doi.org/10.1021/acsearthspacechem.2c00065.

Xuelu Gaoa, S.C., 2008. Petroleum pollution in surface sediments of Daya Bay, South China, revealed by chemical fingerprinting of aliphatic and alicyclic hydrocarbons. Estuar. Coast. Shelf Sci. 80, 95–102.

Yang, Y., Liu, L., Zhang, P., Wu, F., Wang, Y., Xu, C., Zhang, L., An, S., Kuzyakov, Y., 2023. Large-scale ecosystem carbon stocks and their driving factors across Loess Plateau. Carbon Neutrality 2 (1), 5. https://doi.org/10.1007/s43979-023-00044-w.

Yao, F., Johns, W.E., 2010. A HYCOM modeling study of the Persian Gulf: 1. Model configurations and surface circulation. J. Geophys. Res. Oceans 115 (C11). https://doi.org/10.1029/2009JC005781.

Zhang, Y., Su, Y., Liu, Z., Kong, L., Yu, J., Jin, M., 2018. Aliphatic hydrocarbon biomarkers as indicators of organic matter source and composition in surface sediments from shallow lakes along the lower Yangtze River, Eastern China. Org. Geochem. 122, 29–40. https://doi.org/10.1016/j.orggeochem.2018.04.009.

Zhang, X., Ma, F., Dai, Z., Wang, J., Chen, L., Ling, H., Soltanian, M.R., 2022a. Radionuclide transport in multi-scale fractured rocks: a review. J. Hazard. Mater. 424, 127550.

Zhang, X., Wang, Z., Reimus, P., Ma, F., Soltanian, M.R., Xing, B., Dai, Z., 2022b. Plutonium reactive transport in fractured granite: multi-species experiments and simulations. Water Res. 224, 119068.

Zhang, T., Song, B., Han, G., Zhao, H., Hu, Q., Zhao, Y., Liu, H., 2023. Effects of coastal wetland reclamation on soil organic carbon, total nitrogen, and total phosphorus in China: a meta-analysis. Land Degrad. Dev. https://doi.org/10.1002/ldr.4687.